

PHYSIOLOGICAL RESPONSES TO INCREASED TEMPERATURE AND IRRADIANCE IN THE CALCIFYING MACROALGAE, *HALIMEDA MACROLOBA*, *HALIMEDA OPUNTIA* AND *PADINA BORYANA*

BUAPET, P.^{1,2} – SINUTOK, S.^{2,3*}

¹*Division of Biological Science, Faculty of Science, Prince of Songkla University, Hat Yai, Songkhla, 90110 Thailand
(e-mail: pimchanok.b@psu.ac.th)*

²*Coastal Oceanography and Climate Change Research Center, Prince of Songkla University, Songkhla 90110, Thailand*

³*Faculty of Environmental Management, Prince of Songkla University, Hat Yai, Songkhla, 90110, Thailand*

**Corresponding author
e-mail: ssutinee@gmail.com; phone + 66-74-286-847*

(Received 16th May 2023; accepted 1st Aug 2023)

Abstract. Environmental condition varies considerably in intertidal habitat, exposing photosynthetic organisms to diverse stressors, including heat stress and excess light. Herein, we examined the interactive effects of temperature and irradiance on photosynthesis, calcification and oxidative stress in *Halimeda macroloba*, *Halimeda opuntia* and *Padina boryana*, three common calcifying macroalgae in shallow reef flats in Thailand. Six treatments lasting 3 h were established under different temperatures (32, 37, 42°C) and irradiance (150 and 1000 $\mu\text{mol photons m}^{-2} \text{ s}^{-1}$). Net photosynthetic carbon uptake and calcification rates were estimated from changes in pH and total alkalinity, while the quantum yields were assessed using the chlorophyll fluorescence technique. Total reactive oxygen species, superoxide dismutase (SOD) activity, guaiacol peroxidase (GPOX) activity, and total glutathione content were measured at the end of the experiment. Our results show that the stress responses were primarily induced by high temperature, observed as lowered photosynthetic carbon uptake rates, photoinhibition (measured as a decrease in F_v/F_m and $rETR_{\text{max}}$) and lowered calcification rates in all three macroalgae. The most severe effects were observed at 42°C. This extreme temperature also led to the dissolution of calcium carbonate and a reduction in antioxidant capacity (SOD in *H. macroloba*, and *H. opuntia* and GPOX in *P. boryana*). Our findings suggest that a temperature rise is a potential threat to the health of calcified macroalgae. Nevertheless, *H. macroloba* and *H. opuntia* may be more sensitive to heat stress than *P. boryana*, which maintained positive net photosynthetic carbon uptake and calcification rates and higher maximum quantum yield at 42°C.

Keywords: *high temperature, high light intensity, photosynthesis, calcification, oxidative stress*

Introduction

Global climate change has emerged as a pressing issue in recent times, primarily due to escalated human activities and the accumulation of atmospheric greenhouse gases since the pre-industrial era. These factors have contributed to the greenhouse effect, resulting in the absorption of a significant portion of heat energy by the world's oceans. Consequently, there has been a projected increase in the global mean sea surface temperature, leading to more frequent and intense marine heatwaves. Another consequence of elevated carbon dioxide levels is the reduction in oceanic pH, a phenomenon known as ocean acidification (Hough-Guldberg et al., 2018; Pörtner et al.,

2019). These ongoing climate change challenges are anticipated to profoundly impact the structure and functioning of tropical coastal shallow-water communities, including macroalgae (Koch et al., 2013).

Tropical marine calcified macroalgae play a vital role as primary producers within the marine food web through photosynthesis. They also contribute to the production of calcium carbonate (CaCO_3) via calcification, which enhances the formation of reef sediments, promotes accretion and stability, and facilitates the recruitment of coral larvae (Johnson et al., 2014; McNicholl et al., 2020). Moreover, these macroalgae create complex habitats supporting diverse marine organisms (Rees et al., 2017). Recent research has focused on the carbon economy associated with calcified macroalgae. It has been discovered that their calcification process can modify the carbonate chemistry of seawater by releasing CO_2 , resulting in a net loss of atmospheric CO_2 . Intriguingly, this process exhibits diurnal variations due to the close relationship between calcification and photosynthesis (Kalokora et al., 2020; Buapet and Sinutok, 2021).

Elevated temperatures significantly impact various aspects of calcified macroalgae, including photosynthesis, calcification, growth, and biochemical processes (Sinutok et al., 2011, 2012; Prathep et al., 2018; Yucharoen et al., 2021). The specific responses to temperature can vary depending on the species, life forms, functional groups, and interactions with other environmental factors (Kram et al., 2016; Dove et al., 2020; Buapet and Sinutok, 2021). For instance, Campbell et al. (2016) found a positive correlation between photosynthesis and calcification in *Halimeda* species, suggesting that moderate temperature increases can enhance both processes. However, other studies have demonstrated that extreme temperatures can negatively affect calcified macroalgae such as *Halimeda* and *Padina* (Sinutok et al., 2011, 2012; Yucharoen et al., 2021). Temperature also influences diffusion rates and metabolic processes, including oxidative stress, enzyme activity, and active transport, which can impact calcification and photosynthesis (Hurd et al., 2014; Scherner et al., 2016; Marques et al., 2020). Marques et al. (2020) found a reduction of 29.6% in total antioxidant capacity under climate change scenarios for 2100. Additionally, Dove et al. (2020) observed a decline in calcified macroalgal cover, reef accretion, and net ecosystem calcification in reefs exposed to elevated temperatures. Interestingly, recent studies have indicated that non-calcified macroalgae tend to exhibit greater thermotolerance than calcified macroalgae, potentially due to the sensitivity of calcification to thermal stress (Kram et al., 2016; Dove et al., 2020; Yucharoen et al., 2021).

Coastal ecosystems face various stressors, including light stress. Fluctuations in irradiance occur due to factors such as tides, cloud cover, solar angle, and human activities (Hurd et al., 2014). Calcified macroalgae in these ecosystems experience high irradiance during mid-day at low tide, which can lead to photoinhibition, photodamage, and reduced calcification (Harker et al., 1999; Prathep et al., 2018). The interactive effects of multiple stressors can result in complex physiological and ecological responses (Zuñiga-Rios et al., 2014). Studies have shown varying responses of calcified macroalgae to irradiance. For example, Peach et al. (2016) found that irradiance levels ($56\text{--}250 \mu\text{mol photons m}^{-2} \text{s}^{-1}$) did not affect the net calcification rate and crystal microstructure of six *Halimeda* species. However, high irradiance significantly decreased the segment production rate. Similarly, Dutra et al. (2016) observed that the surface area of crustose coralline algae (CCA) significantly declined under high irradiance ($92 \mu\text{mol photons m}^{-2} \text{s}^{-1}$) but doubled in size under low irradiance ($13 \mu\text{mol photons m}^{-2} \text{s}^{-1}$). In contrast, irradiance can enhance calcification in CCA (Dutra et al.,

2016). Prathep et al. (2018) found that calcification and carbon dioxide uptake in *Halimeda macroloba* were promoted by moderate irradiance ($500 \mu\text{mol photons m}^{-2} \text{s}^{-1}$) but inhibited by high irradiance ($1200 \mu\text{mol photons m}^{-2} \text{s}^{-1}$) and high temperature (35°C). The close relationship between photosynthesis and calcification in these species means that a reduction in photosynthesis due to stressors can inhibit calcification and vice versa (Sinutok et al., 2012). These impacts on the carbon balance of calcified macroalgae can have implications for their crucial ecosystem services as primary producers, food security through fisheries, and habitat builders. Moreover, they can also alter their role in the carbon economy (Feely et al., 2004; Anthony et al., 2011).

Halimeda spp. and *Padina* spp. are two significant calcifying macroalgae found in sub-tropical and tropical coastal habitats, including those in Thailand (Sinutok et al., 2008, 2011, 2012; Hill et al., 2015). *Halimeda* spp., which belongs to the Chlorophyta, are highly calcified macroalgae that precipitate CaCO_3 in the intercellular spaces as aragonite. On the other hand, *Padina* spp., which belongs to the Phaeophyta, are lightly calcified macroalgae that deposit aragonite crystals on the cell surface (Kleypas et al., 1999; Hofmann and Bischof, 2014). Previous studies have investigated the extent of CaCO_3 precipitation in different species. For instance, in Phuket, Thailand, the CaCO_3 precipitation in *H. macroloba*, *H. opuntia*, and *P. boryana* was found to be 81%, 77%, and 47%, respectively (Buapet and Sinutok, 2021). In other studies, *P. pavonica*, *P. japonica*, and *P. sanctae-crucis* were found to precipitate CaCO_3 ranging from 9% to 63%, 21%, and 38% of their dry weight, respectively (Okazaki et al., 1986; Johnson and Carpenter, 2012; Hofmann and Bischof, 2014). These variations in calcification characteristics, such as calcification capacity, degree of calcification, calcification site, branching of CaCO_3 polymorphs, and crystal microstructure morphology, as well as their proximity to pH-elevating processes (e.g., photosynthesis, H^+ pumping, carbon-concentrating mechanisms), relative to the external seawater and their microenvironment, can influence the sensitivity, response, and adaptive capacity of these macroalgae to climate change (Borowitzka, 1982; Price et al., 2011; Koch et al., 2013; McNicholl et al., 2020; Buapet and Sinutok, 2021; Schubert et al., 2021). Furthermore, recent research has revealed that under optimal conditions, calcified macroalgae can act as a source of CO_2 , and the degree of CO_2 loss to the atmosphere varies among species. Highly calcified species such as *H. macroloba* and *H. opuntia* exhibited a more significant loss of CO_2 per unit of biomass weight than lightly calcified species like *P. boryana* (Buapet and Sinutok, 2021). However, the way multiple stressors will impact these calcified macroalgae and their carbon economy remains uncertain and contradictory. Therefore, further studies are needed to understand the complex interactions and responses of these macroalgae to multiple stressors, including climate change, and their implications for their carbon balance and overall ecological functioning.

This study investigates the effects of elevated temperature and high light intensity on the physiological processes of three dominant tropical calcified macroalgae: *H. macroloba*, *H. opuntia*, and *P. boryana*, found in the upper sublittoral areas of Phuket, Thailand. Additionally, we aim to understand how these environmental stressors impact the carbon balance within the coastal ecosystem. By conducting this research, we aim to contribute to the existing knowledge on the effects of environmental stressors on calcified macroalgae and gain insights into their role in carbon sequestration and ecosystem functioning. Ultimately, the findings from this study will inform conservation and management efforts, helping to enhance the resilience and ecological integrity of coastal environments in the face of ongoing climate change.

Materials and methods

Halimeda macroloba, *H. opuntia*, and *P. boryana* (n = 84 per species) were hand-collected from the sand flat of Tung Khen Bay, Phuket, Thailand (7.810057; 98.404100), at a depth range of 0.5-1.0 m. Only thalli with intact holdfasts were carefully selected and stored in cool boxes filled with seawater from the sampling site. The samples were promptly transported within 12 h to the aquaria facility of the Coastal Oceanography and Climate Change Research Center at Prince of Songkla University. Seawater was collected in sealed dark polypropylene bottles. Upon arrival at the laboratory, the seawater underwent immediate analysis to determine its pH, salinity, and total alkalinity (TA). The recorded values were as follows: pH = 8.1, salinity = 30, and TA = 2040 ± 50 µM. Phuket, Thailand, experiences an annual sea surface temperature (SST) ranging from 27°C to 32°C. Additionally, the average irradiance at shallow waters in Phuket is approximately 155 µmol photons m⁻² s⁻¹, as reported by Yucharoen et al. (2021).

To minimize any potential influence from microbial activity in the seawater, we prepared sterile seawater in advance, with specific parameters of salinity (30 PSU), pH (8.2), and total alkalinity (TA) (2100 ± 80 µM). Upon arrival at our aquaria facility, the samples were gently rinsed and cleaned using sterile seawater to eliminate any remaining sediment and epiphytes. Subsequently, the samples were placed in aquaria filled with sterile seawater.

To maintain optimal conditions for the samples, we provided constant aeration and irradiance of approximately 150 µmol photons m⁻² s⁻¹, following a 12:12-h light-dark cycle. This was achieved using a compressed air pump and an aquarium LED light (A601, Chihiros, China). The ambient temperatures within the facility ranged from 27°C to 32°C.

To ensure the acclimatization of the samples to the aquaria conditions, a period of 7 days was allowed before commencing the subsequent experiments. During this acclimatization period, regular renewal of the seawater was performed. For our investigation, only algal thalli exhibiting a maximum quantum yield (F_v/F_m) greater than or equal to 0.7, as measured by a pulse amplitude modulated fluorometer (Diving-PAM, Walz, Effeltrich, Germany), were included in the study.

Experimental design

This study aims to examine the impacts of elevated temperature and irradiance on the selected macroalgae species. The temperature and irradiance levels were chosen based on the historical maximum sea surface temperature (32°C), previous research on the optimal temperature for these species, and the average in situ irradiance (Yucharoen et al., 2021).

Six treatments were established, involving different combinations of temperature (32, 37, and 42°C) and irradiance (150 and 1000 µmol photons m⁻² s⁻¹) (see *Fig. 1*). Each treatment was assigned to a temperature-controlled aquarium (immersion thermostat, Lauda, Germany) illuminated by an aquarium LED light (A601, Chihiros, China). Within each aquarium, three 250-mL flasks were placed, with each flask containing one of the macroalgae species (wet weight = 8 g) in 250 ml of sterile seawater. The flasks were supplied with aeration using a compressed air pump and sealed with cling wrap to maintain a closed system.

The experiment consisted of six independent runs ($n = 6$), each lasting 3 h. Seawater was replaced hourly to prevent pH drift from confounding the results (Buapet and Sinutok, 2021). Parameters related to seawater chemistry, such as pH and total alkalinity (TA), were measured at the beginning and at the end of each hour (0, 1, 2, and 3 h, see Fig. 1). These measurements were used to estimate the rates of dissolved inorganic carbon (DIC) uptake and calcification.

The maximum quantum yield (F_v/F_m) was measured at the start (0 h) and end (3 h) of the experiment, while the effective quantum yield of PSII (ϕ_{PSII}) was measured at 1, 2, and 3 h after treatment (see Fig. 1). At the conclusion of the experiment, rapid light curves (RLC) were constructed. Samples were collected by snap freezing the macroalgae in liquid nitrogen and stored in a -80°C freezer for subsequent assessment of oxidative stress activity, including measurements of total reactive oxygen species (ROS) content, superoxide dismutase (SOD) activity, guaiacol peroxidase (GPOX) activity, and glutathione (GSH) content ($n = 6$) (see Fig. 1). Images of the macroalgae at the end of the experiment were captured using a digital camera (Olympus Tough TG-6, Japan). Additionally, photographs of *P. boryana* were taken under a stereo microscope (Leica EZ4, Leica Microsystems (Schweiz) AG, Switzerland) to observe the deposition of calcium carbonate on the surface of the thalli.

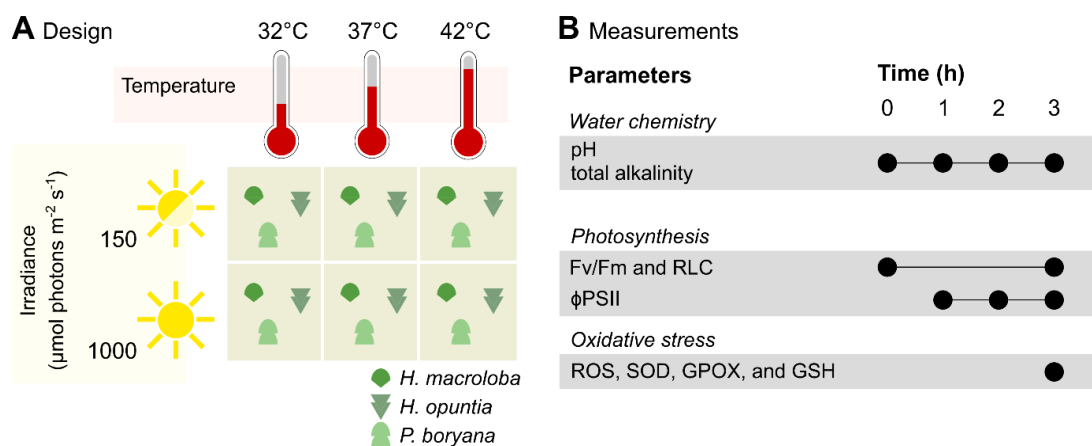


Figure 1. Experimental design (A), investigated parameters and measurement timeline (B)

Determination of seawater pH and total alkalinity and estimation of photosynthetic DIC uptake and calcification rates.

Seawater pH was determined using a benchtop pH meter (Ohaus RL150, Russell, USA). The total alkalinity of the seawater was assessed using a rapid titration method, as described in the work of Buapet et al. (2013). To ensure precision, each measurement was carried out in triplicate to obtain technical replicates

Subsequently, the dissolved inorganic carbon (DIC) encompassing CO_2 , HCO_3^- , and CO_3^{2-} was computed based on the recorded seawater chemistry parameters. This calculation was executed utilizing the CO2SYS.xls software developed by Pierrot and Wallace (2006).

The acquired data were analyzed following the methodologies outlined in Kalokora et al. (2020) and Buapet and Sinutok (2021) to assess the rates of DIC uptake and calcification. To facilitate valid comparisons, the calcification rates were normalized relative to the fresh weight of the macroalgae.

Chlorophyll fluorescence parameters

Photosystem II (PSII) photosynthetic capacity was assessed using a Pulse Amplitude Modulated Fluorometer connected to a 6-mm diameter fiber-optic probe (Diving-PAM, Walz, Effeltrich, Germany). F_v/F_m was measured after a 30-min period of dark adaptation, while measurements of ϕ PSII and rapid light curves (RLCs) were performed under light conditions.

F_v/F_m , representing the maximum quantum yield, was calculated as $(F_m - F_0)/F_m$. Here, F_0 represents the minimum fluorescence of the dark-adapted biological materials, and F_m represents the maximum fluorescence achieved after the application of a saturating pulse.

ϕ PSII, indicating the effective quantum yield of PSII, was calculated as $(F_m - F) / F_m$, where F represents the minimum fluorescence of the light-adapted biological materials. F_m represents the maximum fluorescence achieved after applying a saturating pulse.

RLCs were generated by subjecting the samples to eight increasing irradiances ranging from 45 to 615 $\mu\text{mol photons m}^{-2} \text{ s}^{-1}$, with each irradiance lasting for 20 s. From the RLCs, key parameters such as the maximum relative electron transport rate ($r\text{ETR}_{\text{max}}$), minimum saturating irradiance (E_k), and the initial slope of the light response curve (α) were determined. The calculation of these parameters followed the curve fitting protocols outlined in the works of Platt et al. (1980) and Ralph and Gademann (2005).

Oxidative stress-related parameters

To determine the total content of reactive oxygen species (ROS), a modified DCF test developed by Saewong et al. (2022) was employed. Ground macroalgal tissue weighing 100 mg was homogenized with 1 ml of 10 mM Tris-HCl solution (pH 7.2) and then centrifuged at $12,000 \times g$ for 20 min at 4°C. The resulting supernatant (100 μl) was mixed with 10 μl of 10 mM 2',7'-dichlorofluorescein diacetate (Sigma-Aldrich, USA). After a 10-min incubation in darkness, the fluorescence signal was measured using a fluorescence spectrophotometer (FP-8200, JASCO, Japan) with an excitation wavelength of 504 nm and an emission wavelength of 524 nm. The intensity of the fluorescence signal provided an estimation of the total ROS content in the sample.

Superoxide dismutase (SOD) activity was assessed using a modified NBT (nitroblue tetrazolium) method introduced by Saewong et al. (2022). Ground macroalgal tissue weighing 100 mg was homogenized with 1 ml of extraction buffer composed of 0.2 mM potassium phosphate buffer (pH 7.8) containing 0.1 mM ethylenediaminetetraacetic acid (EDTA). The resulting mixture was then centrifuged at $12,000 \times g$ for 20 min at 4°C. Next, 10 μl of the supernatant was added to a reaction buffer consisting of 200 μl of a solution containing 50 mM phosphate buffer (pH 7.8), 2 mM EDTA, 9.9 mM L-methionine, 55 μM nitroblue tetrazolium, and 0.025% Triton-X100, in duplicate microplates. The reaction was initiated by adding 2 μl of 1 mM riboflavin. One microplate was shielded from light, while the other was exposed to light for 10 min using a 15 W fluorescent tube (Philips, Thailand). Subsequently, the absorbance at 560 nm, which corresponds to the formazan content, was measured using a Biotek spectrophotometer (Vermont, USA). Control measurements were conducted concurrently without the presence of macroalgal extract. SOD activity was estimated by evaluating the relative reduction of formazan due to the inhibitory effect of SOD under light conditions, as described by Saewong et al. (2022).

Guaiacol peroxidase (GPOX) activity was determined following the method modified by Phandee et al. (2022). Extraction was achieved by homogenizing ground macroalgal tissue (100 mg) with 2 ml of extraction buffer (0.1 M Tris–HCl containing 8.75% PVPP, 0.1 M KCl and 0.28% TritonX100) and centrifugation at 4°C and $1520 \times g$ for 30 min. The reaction was initiated by mixing 50 μl of the supernatant with 230 μl of the reaction mixture (50 mM potassium phosphate buffer pH 6.6 containing 1% v/v guaiacol and 0.18% v/v H_2O_2). The absorbance at 470 nm was recorded every 30 s for 5 min (Biotek PowerWaveX, USA), and the slope gave an estimate of GPOX activity.

The content of GSH was measured using a fluorescence-based protocol modified from Nualla-ong et al. (2020). Extraction was achieved by homogenizing ground macroalgal tissue (100 mg) with 200 μl of 25% meta-phosphoric acid (HPO_3) and 1.1 ml of ice-cold extraction buffer (0.1 M sodium phosphate buffer, pH 8.0 containing 5 mM EDTA). The supernatant was collected after centrifugation at $12,000 \times g$ at 4°C for 20 min. The reaction was initiated by combining 90 μl of the supernatant with 1.62 ml of extraction buffer and 90 μl of 1 mg/ml O-Phthalaldehyde (OPT). Total GSH was estimated from the fluorescence signal with an emission at 350 nm and excitation at 420 nm (FP-8200, JASCO, Japan).

Statistical analysis

All the analyses were performed using Statistica academic platform version 13.0 (StatSoft, Tulsa, OK, USA) with a significance level of 95%. Cochran's test was used to verify the assumption of variance homogeneity before conducting the variance analysis (ANOVA).

Repeated-measures ANOVA was used to establish differences in the seawater chemistry (pH and total alkalinity) among temperatures (32, 37 and 42°C) and irradiance levels (150 and 1000 $\mu\text{mol photons m}^{-2} \text{s}^{-1}$) during each hour of incubation. Sampling time was used as a within-group factor (initial and final).

The difference in photosynthetic DIC uptake, calcification rates, and effective quantum yield (ϕPSII) was analyzed using repeated-measures ANOVA with each hour of incubation set as a within-group factor. The difference in the maximum quantum yield (F_v/F_m) obtained after dark adaptation was analyzed using repeated-measures ANOVA with the time of measurement (before and after the exposure to experimental condition) set as a within-group factor.

Two-way ANOVA was used to establish differences in the oxidative stress-related parameters among temperatures (32, 37 and 42°C) and irradiance levels (150 and 1000 $\mu\text{mol photons m}^{-2} \text{s}^{-1}$) at the end of the experiment. Each species was tested separately.

Multiple comparison tests were performed using Tukey's honestly significant difference (HSD) test.

The relationships between photosynthesis and calcification were analyzed by linear regression.

Results

The results revealed a significant alteration in seawater chemistry upon incubation with macroalgae, as illustrated in *Figure 2A, B* (refer to the ANOVA results in *Tables A1–A6* in the *Appendix*). During each incubation interval, an increase in seawater pH was observed (*Fig. 2A*, Tukey's HSD test). Total alkalinity decreased at

32°C and 37°C but increased at 42°C (Fig. 2A). These changes were primarily influenced by temperature (Repeated-measure ANOVA) and the interaction between temperature and incubation time (Repeated-measure ANOVA). Notably, the impact of irradiance on seawater chemistry was not found to be significant, except for seawater pH in the treatments involving *Halimeda macroloba* and *H. opuntia* during the final hour of incubation (Repeated-measure ANOVA).

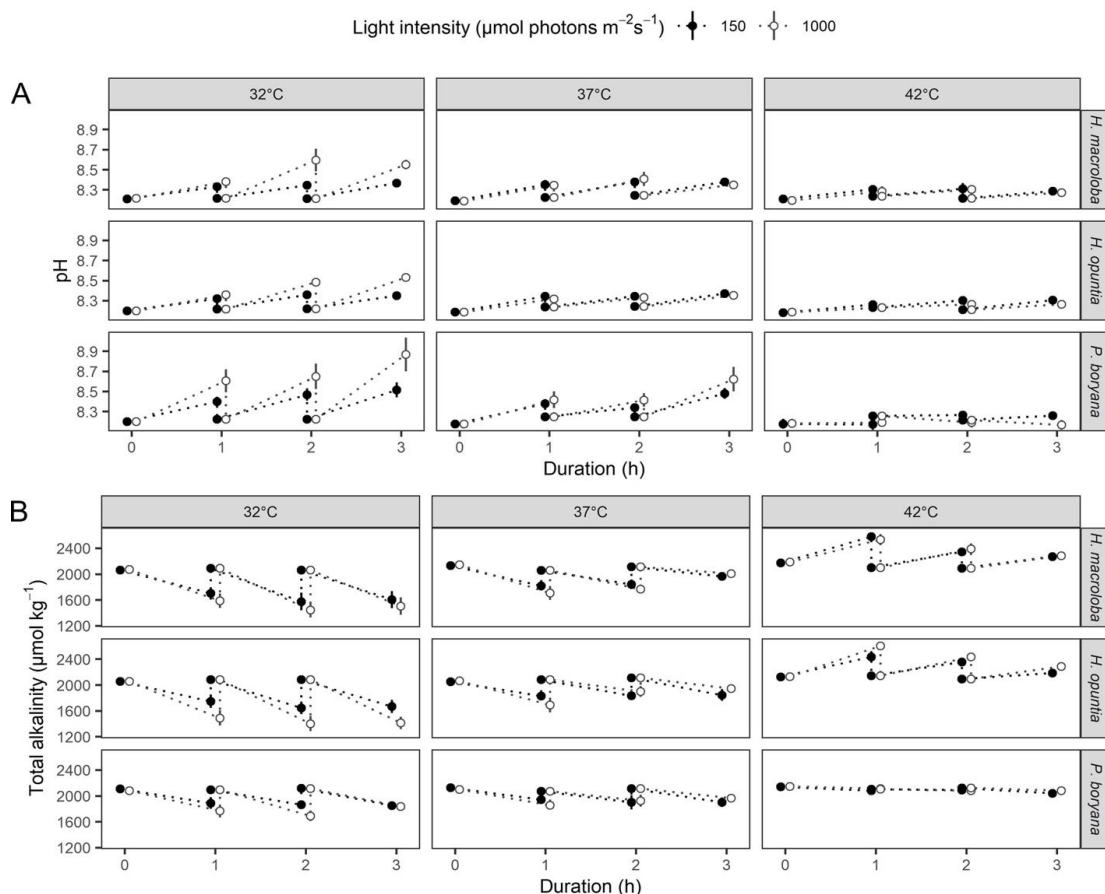


Figure 2. Hourly change in seawater chemistry: pH (A) and total alkalinity (B) after incubation with *Halimeda macroloba*, *Halimeda opuntia* and *Padina boryana* in different temperatures and irradiance treatments. Data are means \pm SE

The variations in dissolved inorganic carbon (DIC) uptake rates and calcification rates among the three macroalgae were evident in response to the different treatments, as depicted in Figure 3A, B (refer to the ANOVA results in Tables A7–A8). These effects were primarily influenced by temperature (Repeated-measure ANOVA). Specifically, incubation at 42°C significantly impacted DIC uptake and calcification rates in all tested macroalgae, with *H. macroloba* and *H. opuntia* exhibiting net DIC loss and dissolution. There was a significant effect of temperature and a significant interaction between incubation time and temperature regarding DIC uptake rates in *H. macroloba* (Fig. 3A, Repeated-measure ANOVA). In the case of *H. opuntia*, significant effects of incubation time, temperature, and the interaction between temperature and irradiance on DIC uptake rates were observed (Fig. 3A, Repeated-measure ANOVA).

Moreover, significant temperature and incubation time effects were noted for DIC uptake rates in *P. boryana* (Fig. 3A, Repeated-measure ANOVA). Regarding calcification rates, *H. macroloba* and *H. opuntia* exhibited variations dependent on the interaction between incubation time and temperature (Fig. 3B, Repeated-measure ANOVA), while *P. boryana* showed variations dependent on temperature alone (Fig. 3B, Repeated-measure ANOVA).

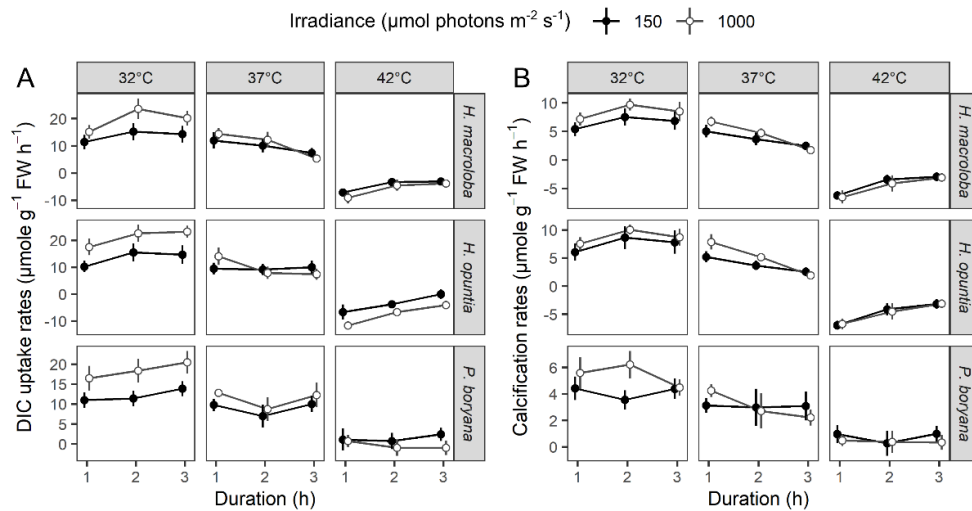


Figure 3. Photosynthetic DIC uptake (A) and calcification rates (A) of *Halimeda macroloba*, *Halimeda opuntia* and *Padina boryana* in different temperatures and irradiance treatments. Data are means \pm SE

Significant interactions between temperature and irradiance were observed concerning the effective quantum yield (Φ PSII) of all three macroalgae, as presented in Figure 4 (refer to the ANOVA results in Table A9). Under light conditions, samples exposed to 150 $\mu\text{mol photons m}^{-2} \text{s}^{-1}$ exhibited higher Φ PSII than those exposed to 1000 $\mu\text{mol photons m}^{-2} \text{s}^{-1}$ (Tukey's HSD test). However, this effect was attenuated when the macroalgae were incubated at 42°C (Fig. 4). Furthermore, significant interactions among temperature, irradiance, and incubation time were found to affect the maximum quantum yield (F_v/F_m) in *H. macroloba* (Fig. 4, see ANOVA results in Table A10). For *H. opuntia* and *P. boryana*, significant effects of temperature, irradiance, and incubation time were observed (Repeated-measure ANOVA), although no significant interaction between these two stressors was detected. At 32 and 37°C, the final F_v/F_m values of samples exposed to 1000 $\mu\text{mol photons m}^{-2} \text{s}^{-1}$ were lower than the initial values and lower than the final F_v/F_m values of samples exposed to 150 $\mu\text{mol photons m}^{-2} \text{s}^{-1}$ (Tukey's HSD test). At 42°C, the final F_v/F_m values were lower than the initial values, but the predominant effects were driven by heat stress (Tukey's HSD test).

The light energy utilization of the three macroalgae, as assessed by rapid light curves, was influenced by increases in temperature and irradiance (Tables 1 and A11–A13). Incubation at 42°C reduced the maximum relative electron transport rates ($r\text{ETR}_{\text{max}}$) across all species, while an increase in temperature led to a gradual decline in alpha values (Table 1, Tukey's HSD test). The saturating irradiance (E_k) generally increased with rising temperature, except for *P. boryana*, where no significant difference was observed (Table 1).

Table 1. Photosynthetic parameters of *Halimeda macroloba*, *Halimeda opuntia* and *Padina boryana* derived from rapid light curves (mean \pm SE, $n = 6$). Values for each variable with the same letter are not significantly different at $p = 0.05$ (Tukey's HSD test)

Parameters		150 $\mu\text{mol photons m}^{-2} \text{s}^{-1}$	1000 $\mu\text{mol photons m}^{-2} \text{s}^{-1}$
rETR _{max}	<i>Halimeda macroloba</i>		
	- 32°C	15.25 \pm 1.23 ^{ab}	14.69 \pm 2.60 ^{ab}
	- 37°C	8.59 \pm 0.54 ^{bc}	21.66 \pm 1.50 ^a
	- 42°C	3.80 \pm 1.52 ^c	4.96 \pm 1.76 ^c
	<i>Halimeda opuntia</i>		
	- 32°C	13.71 \pm 2.82 ^{ab}	16.68 \pm 2.36 ^{ab}
	- 37°C	11.41 \pm 4.00 ^{ab}	15.99 \pm 1.19 ^a
	- 42°C	5.29 \pm 1.64 ^b	9.01 \pm 0.70 ^{ab}
	<i>Padina boryana</i>		
	- 32°C	56.73 \pm 4.14 ^a	46.60 \pm 19.50 ^a
	- 37°C	36.11 \pm 0.88 ^a	49.12 \pm 10.36 ^a
	- 42°C	21.90 \pm 4.00 ^b	18.43 \pm 4.84 ^b
Alpha	<i>Halimeda macroloba</i>		
	- 32°C	0.34 \pm 0.01 ^a	0.26 \pm 0.01 ^b
	- 37°C	0.20 \pm 0.03 ^b	0.07 \pm 0.01 ^c
	- 42°C	0.01 \pm 0.01 ^c	0.02 \pm 0.01 ^c
	<i>Halimeda opuntia</i>		
	- 32°C	0.35 \pm 0.03 ^a	0.25 \pm 0.03 ^b
	- 37°C	0.16 \pm 0.03 ^{bc}	0.08 \pm 0.00 ^{cd}
	- 42°C	0.02 \pm 0.01 ^d	0.04 \pm 0.01 ^d
	<i>Padina boryana</i>		
	- 32°C	0.27 \pm 0.01 ^a	0.23 \pm 0.01 ^{ab}
	- 37°C	0.27 \pm 0.02 ^a	0.17 \pm 0.03 ^{bc}
	- 42°C	0.10 \pm 0.01 ^{cd}	0.08 \pm 0.02 ^d
E _k	<i>Halimeda macroloba</i>		
	- 32°C	44.92 \pm 5.54 ^a	56.83 \pm 7.98 ^a
	- 37°C	46.19 \pm 10.74 ^a	316.67 \pm 56.27 ^b
	- 42°C	524.52 \pm 299.86 ^b	252.29 \pm 39.65 ^b
	<i>Halimeda opuntia</i>		
	- 32°C	40.40 \pm 10.78 ^a	71.95 \pm 17.15 ^{ab}
	- 37°C	81.98 \pm 41.13 ^{ab}	208.66 \pm 21.74 ^b
	- 42°C	200.62 \pm 67.93 ^b	254.41 \pm 34.39 ^b
	<i>Padina boryana</i>		
	- 32°C	215.60 \pm 20.31 ^a	211.95 \pm 92.60 ^a
	- 37°C	133.54 \pm 8.61 ^a	282.62 \pm 191.07 ^a
	- 42°C	223.52 \pm 25.54 ^a	231.51 \pm 25.43 ^a

Regression analysis revealed a positive correlation between DIC uptake rates and calcification rates ($p < 0.001$) in all macroalgae (see *Table A14*). The intercepts were negative (<0) in *H. macroloba* and *H. opuntia*, while they were positive (>0) in *P. boryana*. However, this relationship was less evident when examining the association between relative electron transport rates and calcification rates (*Fig. 5*; *Table A15*). A significant positive relationship ($p < 0.001$) was found in *H. macroloba* during the first and second hours of incubation, as well as in *H. opuntia* during the first hour of incubation.

The three macroalgae exhibited diverse responses related to oxidative stress, as depicted in *Figure 6A-D* (refer to ANOVA results in *Tables A16–A19*). Total reactive oxygen species (ROS, *Fig. 6A*) exhibited variations depending on temperature (Two-way ANOVA). Incubation at 42°C decreased ROS accumulation in *H. macroloba* and *H. opuntia*, while it increased ROS accumulation in *P. boryana* (Tukey's HSD test). SOD activity (*Fig. 6B*) decreased with increasing temperature in *H. macroloba* and *H. opuntia* (Two-way ANOVA). In terms of guaiacol peroxidase (GPOX) activity (*Fig. 6C*, only *P. boryana* showed an interaction between temperature and irradiance (Two-way ANOVA). At 42°C, GPOX activity decreased in *P. boryana* exposed to 1000 $\mu\text{mol photons m}^{-2} \text{s}^{-1}$. Lastly, total glutathione content increased with increasing irradiance in *P. boryana* (*Fig. 6D*, Tukey's HSD test).

Figure 7 illustrates the macroalgal thalli appearance after 3 h in the experimental conditions. *Halimeda macroloba* (*Fig. 7A-F*) and *H. opuntia* (*Fig. 7G-L*) did not exhibit signs of bleaching, although the thalli exposed to 37 and 42°C appeared slightly paler compared to those exposed to 32°C. In the case of *P. boryana*, partial dissolution was observed in thalli exposed to 37 and 42°C (*Fig. 7M-R*). This observation was further confirmed by using a stereomicroscope, which revealed the absence of some calcified bands (*Fig. 7S-X*).

Discussion

The findings of this study highlight that heat stress had more detrimental effects on the physiological performance of *Halimeda macroloba*, *H. opuntia*, and *Padina boryana* compared to high irradiance. This was evident in various aspects, including photosynthetic attributes such as net inorganic carbon uptake rates, F_v/F_m (maximum quantum yield of photosystem II), and $rETR_{\text{max}}$ (maximum relative electron transport rates), as well as calcification rates. The antioxidant capacity of the tested macroalgae was also compromised under heat stress. These stress responses were observed at 37°C and became more severe at 42°C. Notably, significant interactive effects between high-temperature and high-irradiance treatments were observed only in the ΦPSII (effective quantum yield of photosystem II) of all species, the F_v/F_m of *H. macroloba*, and the guaiacol peroxidase (GPOX) activity of *P. boryana*.

The influence of high temperature as a stressor surpasses that of other factors, such as high light intensity and ocean acidification, as highlighted in studies by Ralph (1999), Graba-Landry et al. (2018), Costa et al. (2021), and Saewong et al. (2022). The impact of elevated temperature on primary metabolism, particularly photosynthesis, has been extensively documented in various marine photosynthetic organisms (Fujimoto et al., 2015; Scherner et al., 2016; Prathep et al., 2018; Yang et al., 2021; Yucharoen et al., 2021). In line with these findings, our results reveal that warming affects both carbon assimilation and the photosynthetic light reactions in all tested species.

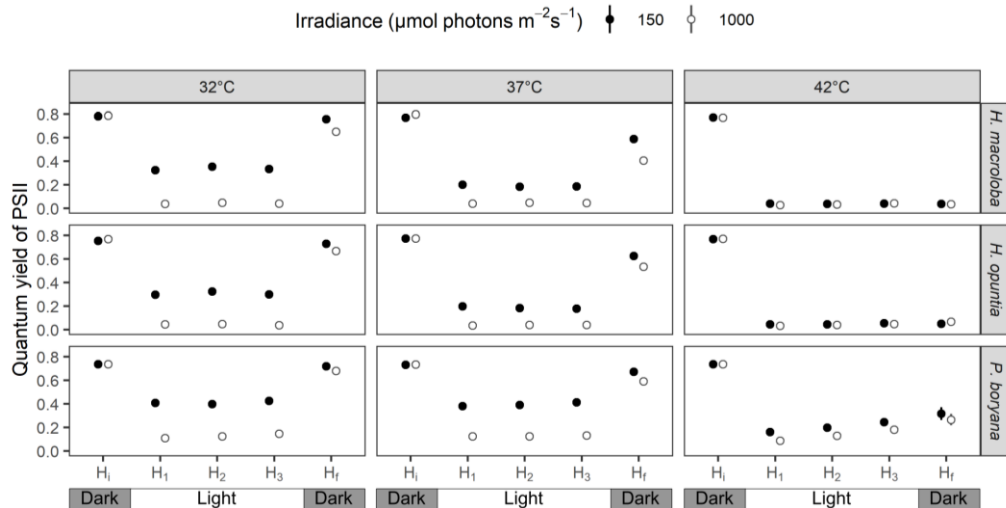


Figure 4. The maximum quantum yield (measured in darkness) and the effective quantum yield (measured under ambient light) of *Halimeda macroloba*, *Halimeda opuntia* and *Padina boryana* in different temperatures and irradiance treatments. Data are means \pm SE

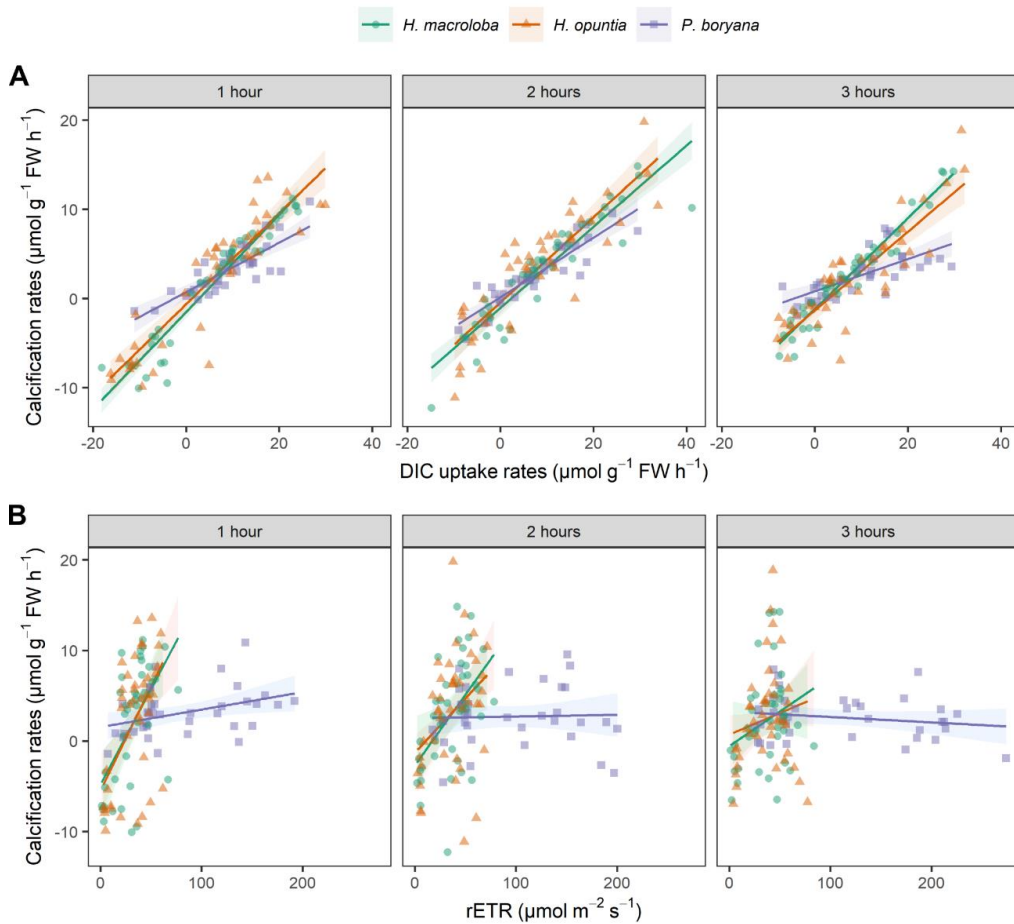


Figure 5. Relationship between photosynthetic DIC uptake rates and calcification rates (A) and between relative electron transport rates (rETR) and calcification rates (B) of *Halimeda macroloba*, *Halimeda opuntia* and *Padina boryana*. Data are obtained from calculations shown in Figures 3 and 4

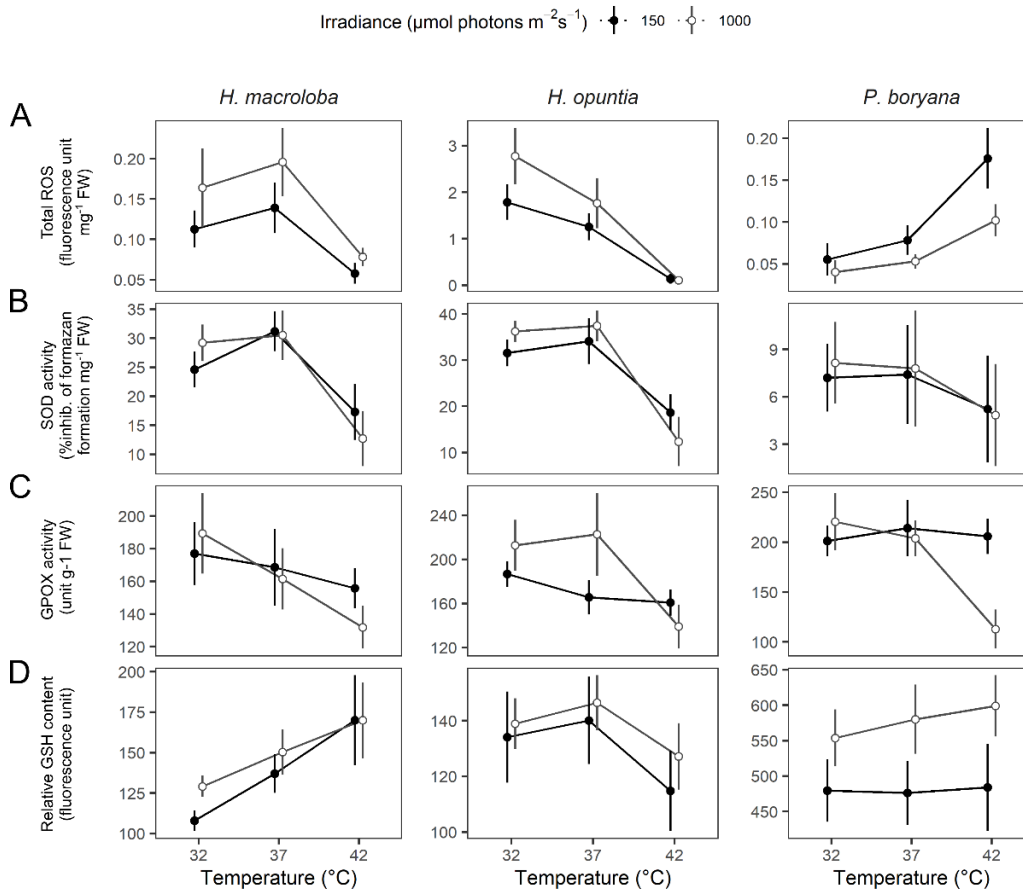


Figure 6. Oxidative stress-related parameters: total reactive oxygen species (A), the activity of superoxide dismutase (B), the activity of guaiacol peroxidase (C) and glutathione content (D) in *Halimeda macroloba*, *Halimeda opuntia* and *Padina boryana* exposed to 3 hours of different temperatures and irradiances

As temperatures reach 37°C, we observed a more pronounced decline in photosynthetic activity compared to cellular respiration. This led to a decrease in net dissolved inorganic carbon (DIC) uptake (Tait and Schiel, 2013; Fujimoto et al., 2015; Ji et al., 2016; Rasmusson et al., 2020). This reduction in DIC uptake is associated with a less steep rise in seawater pH (Fig. 2). Furthermore, the detection of net DIC release suggests that a negative carbon balance may occur in *H. macroloba* and *H. opuntia* at 42°C. Although the high temperature is likely to inhibit the activity of Rubisco, the key enzyme involved in photosynthetic carbon fixation (Demirevska-Kepova and Feller, 2004), our results indicate that photoinhibition of the light reactions also contributes to the reduced photosynthetic performance, as evidenced by a decline in chlorophyll fluorescence parameters.

The heat-sensitive components of photosynthetic light reactions, such as the photosystem II D1 protein and oxygen-evolving complex, may undergo degradation or disassociation under high-temperature conditions, resulting in a significant decrease in effective quantum yield of photosystem II (ΦPSII), maximum quantum yield of photosystem II (F_v/F_m), and maximum relative electron transport rates ($r\text{ETR}_{\text{max}}$) observed at 42°C (Kumar et al., 2020; Yang et al., 2021). These findings highlight the vulnerability of the photosynthetic apparatus to heat stress and provide insights into the underlying mechanisms contributing to the observed decline in photosynthetic performance.

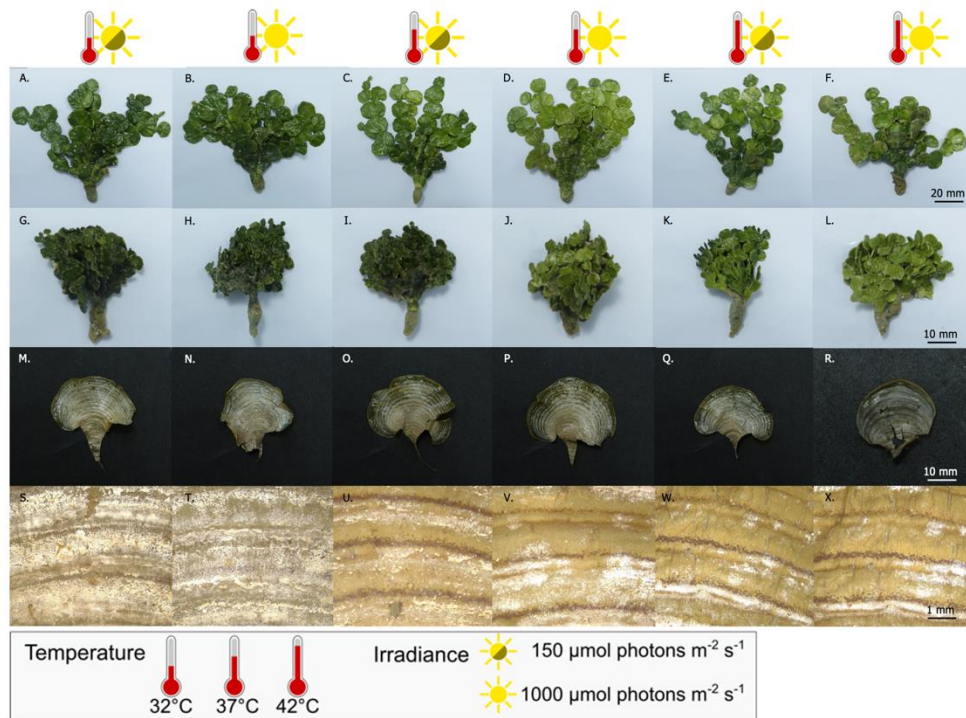


Figure 7. *Halimeda macroloba* (A–F), *Halimeda opuntia* (G–L), and *Padina boryana* (M–R) after 3 h in experimental conditions. Photographs of *Padina boryana* taken under a stereo microscope (S–X) showing deposition of calcium carbonate on the surface of thalli

The decline in calcification observed in the three macroalgae with increasing temperature aligns with findings from other studies on calcified marine organisms (Sinutok et al., 2011; Yang et al., 2021; Ross et al., 2022). The sensitivity of calcification to heat stress may be attributed to various biological processes, including energy imbalance and gene expression regulation (Yang et al., 2021; Ross et al., 2022), the involvement of enzymes in calcification (Schermer et al., 2016; Marques et al., 2020), and geochemical processes influenced by the surrounding conditions (Barry et al., 2013; Gao et al., 2019). In our study, the decreased calcification at 37°C and the observed dissolution of calcium carbonate (CaCO_3) at 42°C cannot be solely attributed to seawater acidification. While the influence of seawater chemistry on calcification cannot be completely ruled out, it is essential to consider other factors, such as the calcifying fluid chemistry in *Halimeda* spp. (De Beer and Larkum, 2001), that may contribute to the observed effects. The complex interplay between biological and geochemical processes underscores the multifaceted nature of calcification responses to high temperatures and highlights the need for further investigation into the underlying mechanisms.

In contrast to previous reports (Figueroa et al., 2014; Gouvêa et al., 2017), our study reveals a decrease in the antioxidant capacity of the three macroalgae under heat stress conditions. The observed reduction in superoxide dismutase (SOD) activity in *H. macroloba* and *H. opuntia* at 42°C is likely a result of heat-induced degradation, as described by Sainz et al. (2010). While SOD is an important frontline defense against oxidative stress (Sainz et al., 2010), the lower SOD activity in these two macroalgae did not lead to an overaccumulation of reactive oxygen species (ROS), but rather a

depletion of ROS in the case of *H. opuntia*. A similar reduction in ROS accumulation was observed in the macroalga *Ulva intestinalis* after exposure to 40°C for 4 h (Saewong et al., 2021). It is worth noting that macroalgae can release ROS as a response to injury caused by grazing (McDowell et al., 2014). The possibility of heat-induced injury and subsequent release of ROS to explain the lower ROS levels in heat-stressed *H. opuntia* remains to be experimentally tested. Therefore, our findings suggest that total ROS may not be an accurate biomarker for assessing heat stress in *H. macroloba* and *H. opuntia*. In contrast, we observed a higher accumulation of ROS in response to increasing temperature in *P. boryana*. Additionally, guaiacol peroxidase (GPOX) activity was inhibited in this species when incubated at 42°C under 1000 $\mu\text{mol photons m}^{-2} \text{s}^{-1}$. Surprisingly, this inhibition did not exacerbate photoinhibition or lead to increased ROS accumulation, suggesting that other antioxidative enzymes may be able to compensate for the lack of GPOX under these conditions.

Although the effects were relatively minor, light modulated certain physiological responses in the three macroalgae. An irradiance of 1000 $\mu\text{mol photons m}^{-2} \text{s}^{-1}$ increased the photosynthetic DIC uptake of *H. opuntia* at 32°C, indicating that light availability was a limiting factor for their photosynthetic DIC uptake when heat stress was absent. Surprisingly, we did not observe any significant changes in calcification rates influenced by irradiance, which contradicts a study by Wei et al. (2020) that showed enhanced calcification in *Halimeda cylindracea* and *H. lacunalis* with increasing irradiance. Similarly, Prathep et al. (2018) observed light-stimulated calcification in *H. macroloba* when irradiance rose from 50 to 500 $\mu\text{mol photons m}^{-2} \text{s}^{-1}$ but not when irradiance exceeded 500 $\mu\text{mol photons m}^{-2} \text{s}^{-1}$. It is possible that the irradiance levels used in our study exceeded the saturating irradiance for calcification in these macroalgae.

In all three species, exposure to 1000 $\mu\text{mol photons m}^{-2} \text{s}^{-1}$ at 32°C and 37°C resulted in a decrease in ΦPSII , indicating reversible inactivation of photosystem II (PSII). This phenomenon, known as dynamic photoinhibition, has been observed in macroalgae exposed to high irradiance during low tides and is considered a protective mechanism against photooxidative stress (Harker et al., 1999; Figueroa et al., 2009; Betancor et al., 2015). The reversible nature of dynamic photoinhibition was confirmed by the recovery of the quantum yield after dark adaptation, measured as F_v/F_m . However, the incomplete recovery of ΦPSII implies that high irradiance may have induced a certain degree of chronic photoinhibition at 32°C and 37°C. Further investigations with prolonged dark adaptation are recommended to better understand the extent and persistence of chronic photoinhibition under these conditions.

Padina boryana was the only species in our study that exhibited varied antioxidant responses depending on the light environment. Previous studies have demonstrated rapid accumulation of glutathione (GSH) in response to high light intensity in the model plant *Arabidopsis*, where GSH plays a crucial role in light-induced rapid gene regulation (Choudhury et al., 2018; König et al., 2018). Other studies on macroalgae, such as *Ulva fasciata* (Shiu and Lee, 2005) and *Gracilaria tenuistipitata* (Bonomi-Barufi et al., 2020), have highlighted the involvement of GSH in UV radiation tolerance through the AsA-GSH cycle and the activity of glutathione peroxidase, respectively. These findings underscore the significance of GSH in stress tolerance mechanisms in macroalgae. However, it is essential to note that ambient light levels in tropical intertidal areas, especially during midday, can exceed 1000 $\mu\text{mol photons m}^{-2} \text{s}^{-1}$ (Buapet et al., 2017; Yucharoen et al., 2021). Therefore, interactions among multiple stressors may lead to different physiological responses under stronger irradiance conditions.

Photosynthesis and calcification in calcified macroalgae are closely interconnected processes (De Beer and Larkum, 2001; McNicholl et al., 2019; Kalokora et al., 2020; Buapet and Sinutok, 2021). Consistent with our previous findings (Buapet and Sinutok, 2021), we observed positive relationships between net dissolved inorganic carbon (DIC) uptake and calcification rates in *H. macroloba*, *H. opuntia*, and *P. boryana*. However, when using the photosynthetic electron transport rate as a proxy for photosynthesis, the interrelation between photosynthesis and calcification became less apparent. While it has been established that light and functional photosynthetic electron transport is necessary for the calcification process (De Beer and Larkum, 2001; Buapet and Sinutok, 2021; McNicholl and Koch, 2021), our study did not find a direct association between electron transport rates and calcification rates.

These results suggest that factors related to photosynthetic DIC uptake, such as an increase in pH and the saturation state of calcium carbonate (CaCO_3), may be the critical drivers of calcification (De Beer and Larkum, 2001). The decoupling of photosynthetic electron transport and carbon fixation has been observed in various marine photosynthetic organisms under environmental stress, attributed to alternative electron flows and state transitions (Ihnken et al., 2014; Oakley et al., 2014; Buapet and Björk, 2016; Prathep et al., 2018). In our study, this decoupling could explain the lack of a relationship between electron transport and calcification rates. Additionally, the regulation of calcification and photosynthetic carbon fixation processes may involve independent heat-sensitive pathways, such as photorespiration, carbonic anhydrase-catalyzed reactions, and proton pumps (McNicholl and Koch, 2021; Yang et al., 2021; Zuñiga-Rios et al., 2021).

The stress responses observed in our study indicate that the high temperatures used exceeded the physiological thresholds of the three macroalgae. Consistent with previous research on macroalgae and other marine photosynthetic organisms (Munoz et al., 2018; Román et al., 2020; Ho et al., 2021; Yang et al., 2021; Yucharoen et al., 2021), temperatures outside their tolerance ranges can have adverse effects at various levels of biological organization. While short-term physiological responses may not directly translate into long-term fitness and acclimation capacity, they can serve as indicators of sensitivity to warming scenarios. Our experiment observed that the tested species exhibited different thermotolerance capacities, with *P. boryana* showing greater resilience compared to *H. macroloba* and *H. opuntia*. The higher thermotolerance of *P. boryana* was evident from the lesser degree of DIC release and calcium carbonate dissolution observed at 42°C, as well as the partial recovery of F_v/F_m after exposure to that temperature. These findings underscore the importance of further investigating the underlying mechanisms responsible for the differential thermotolerance among these macroalgae.

Our findings highlight the species-specific sensitivity and response of the three common calcified macroalgae to heat stress and high irradiance, indicating that these responses vary due to their calcification characteristics. Although the seawater temperatures employed in our study exceed historical sea surface temperatures documented in databases (<https://podaac.jpl.nasa.gov/dataset/MUR-JPL-L4-149GLOB-v4.1>) and reported in the scientific literature (Tanzil et al., 2009; Yucharoen et al., 2021), it is essential to acknowledge that in-situ temperatures can reach above 40°C in certain tropical intertidal areas. This has been documented in studies by Collier and Waycott (2014), Pederson et al. (2016), and George et al. (2018). Considering that photosynthesis and calcification, the fundamental processes of *H. macroloba*, *H.*

opuntia, and *P. boryana*, are significantly impacted by increasing temperatures within the potential range found in their natural habitats, it is essential to incorporate temperature considerations into monitoring and preventive strategies. This approach is necessary to ensure the future health and resilience of calcified macroalgae in intertidal environments. Given that these calcified macroalgae can act as a source of CO₂ and the degree of CO₂ loss to the atmosphere differs among species (Buapet and Sinutok, 2021), these individual responses will have implications for their carbon economy and the overall carbon budget of the coastal ecosystem.

Conclusion

In conclusion, our study demonstrates the vulnerability of calcified macroalgae to high temperatures, particularly at 42°C. This temperature led to a number of negative effects, including reduced photosynthesis, decreased calcification, calcium carbonate dissolution, and compromised antioxidant capacity. These findings suggest that extreme temperatures pose a significant threat to calcified macroalgae, and that different species may vary in their vulnerability to climate change-related stressors. Our findings contribute valuable insights for the conservation and management of coastal ecosystems, and emphasize the need to address the impacts of climate change on calcifying macroalgae.

Acknowledgements. This research was funded by the National Science, Research and Innovation Fund (NSRF) and Prince of Songkla University, grant number SCI6506095M. We thank Coastal Oceanography and Climate Change Research Center (COCC), Prince of Songkla University (PSU), Faculty of Environmental Management, PSU and Division of Biological Science, Faculty of Science, PSU for research facilities.

REFERENCES

- [1] Anthony, K. R. N., Kleypas, A. J., Gattuso, J.-P. (2011): Coral reefs modify their seawater carbon chemistry - implications for impacts of ocean acidification. – *Global Change Biology* 17(12): 3655-3666. DOI: 10.1111/j.1365-2486.2011.02510.x.
- [2] Barry, S. C., Frazer, T. K., Jacoby, C. A. (2013): Production and carbonate dynamics of *Halimeda incrassata* (Ellis) Lamouroux altered by *Thalassia testudinum* Banks and Soland Ex König. – *Journal of Experimental Marine Biology and Ecology* 444: 73-80. DOI: 10.1016/j.jembe.2013.03.012.
- [3] Betancor, S., Domínguez, B., Tuya, F., Figueroa, F. L., Haroun, R. (2015): Photosynthetic performance and photoprotection of *Cystoseira humilis* (Phaeophyceae) and *Digenea simplex* (Rhodophyceae) in an intertidal rock pool. – *Aquatic Botany* 121: 16-25. <https://doi.org/10.1016/j.aquabot.2014.10.008>.
- [4] Bonomi-Barufi, J., Figueroa, F. L., Korbee, N., Momoli, M. M., Martins, A. P., Colepicolo, P., Van Sluys, M.-A., Oliveira, M. C. (2020): How macroalgae can deal with radiation variability and photoacclimation capacity: the example of *Gracilaria tenuistipitata* (Rhodophyta) in laboratory. – *Algal Research* 50: 102007. <https://doi.org/10.1016/j.algal.2020.102007>.
- [5] Borowitzka, M. A. (1982): Morphological and cytological aspects of algal calcification. – *International Review of Cytology-a Survey of Cell Biology* 74: 127-162. [https://doi.org/10.1016/S0074-7696\(08\)61171-7](https://doi.org/10.1016/S0074-7696(08)61171-7).

- [6] Buapet, P., Björk, M. (2016): The role of O₂ as an electron acceptor alternative to CO₂ in photosynthesis of the common marine angiosperm *Zostera marina* L. – *Photosynthesis Research* 129: 59-69. DOI: 10.1007/s1120-016-0268-4
- [7] Buapet, P., Sinutok, S. (2021): Calcification in three common calcified algae from Phuket, Thailand: potential relevance on seawater carbonate chemistry and link to photosynthetic process. – *Plants* 10(11): 2537. DOI: 10.3390/plants10112537.
- [8] Buapet, P., Gullström, M., Björk, M. (2013): Photosynthetic activity of seagrasses and macroalgae in temperate shallow waters can alter seawater pH and total inorganic carbon content at the scale of a coastal embayment. – *Marine and Freshwater Research* 64(11): 1040-1048. DOI: 10.1071/MF12124.
- [9] Buapet, P., Makkliang, F., Thammakhet-Buranachai, C. (2017): Photosynthetic activity and photoprotection in green and red leaves of the seagrasses, *Halophila ovalis* and *Cymodocea rotundata*: implications for the photoprotective role of anthocyanin. – *Marine Biology* 164: 182. <https://doi.org/10.1007/s00227-017-3215-9>.
- [10] Campbell, J. E., Fisch, J., Langdon, C., Paul, V. J. (2016): Increased temperature mitigates the effects of ocean acidification in calcified green algae (*Halimeda* Spp.). – *Coral Reefs* 35: 357-368. DOI: 10.1007/s00338-015-1377-9.
- [11] Choudhury, F. K., Devireddy, A. R., Azad, R. K., Shulaev, V., Mittler, R. (2018): Rapid accumulation of glutathione during light stress in *Arabidopsis*. – *Plant and Cell Physiology* 59(9): 1817-1826. <https://doi.org/10.1093/pcp/pcy101>.
- [12] Collier, C. J., Waycott, M. (2014): Temperature extremes reduce seagrass growth and induce mortality. – *Marine Pollution Bulletin* 83(2): 483-490. DOI: 10.1016/j.marpolbul.2014.03.050.
- [13] Costa, M. M., Silva, J., Barrote, I., Santos, R. (2021): Heatwave effects on the photosynthesis and antioxidant activity of the seagrass *Cymodocea nodosa* under contrasting light regimes. – *Oceans* 2: 448-460. DOI: 10.3390/oceans2030025.
- [14] De Beer, D., Larkum, A. W. D. (2001): Photosynthesis and calcification in the calcifying algae *Halimeda discoidea* studied with microsensors. – *Plant Cell and Environment* 24(11): 1209-1217. DOI: 10.1046/j.1365-3040.2001.00772.x.
- [15] Demirevska-Kepova, K., Feller, U. (2004): Heat sensitivity of rubisco, rubisco activase and rubisco binding protein in higher plants. – *Acta Physiologiae Plantarum* 26: 103-114. <https://doi.org/10.1007/s11738-004-0050-7>.
- [16] Dove, S. G., Brown, K. T., Van Den Heuvel, A., Chai, A., Hoegh-Guldberg, O. (2020): Ocean warming and acidification uncouple calcification from calcifier biomass which accelerates coral reef decline. – *Communications Earth & Environment* 1(1): 55. DOI: 10.1038/s43247-020-00054-x.
- [17] Dutra, E., Koch, M., Peach, K., Manfrino, C. (2016): Tropical crustose coralline algal individual and community responses to elevated pCO₂ under high and low irradiance. – *ICES Journal of Marine Science* 73(3): 803-813. <https://doi.org/10.1093/icesjms/fsv213>.
- [18] Feely, R. A., Sabine, C. L., Lee, K., Berelson, W., Kleypas, J., Fabry, V. J., Millero, F. J. (2004): Impact of anthropogenic CO₂ on the CaCO₃ system in the oceans. – *Science* 305(5682): 362-6. DOI: 10.1126/science.1097329.
- [19] Figueroa, F., Martínez, B., Israel, A., Neori, A., Malta, E., Ang, P., Inken, S., Marquardt, R., Rachamim, T., Arazi, U., Frenk, S., Korbee, N. (2009): Acclimation of red sea macroalgae to solar radiation: photosynthesis and thallus absorptance. – *Aquatic Biology* 7(1): 159-172. DOI: 10.3354/ab00186.
- [20] Figueroa, F. L., Domínguez-González, B., Korbee, N. (2014): Vulnerability and acclimation to increased UVB radiation in three intertidal macroalgae of different morpho-functional groups. – *Marine Environmental Research* 97: 30-38. DOI: 10.1016/j.marenvres.2014.01.009.
- [21] Fujimoto, M., Nishihara, G. N., Prathep, A., Terada, R. (2015): The Effect of irradiance and temperature on the photosynthesis of an Agarophyte, *Gelidiella acerosa* (Gelidiales,

- Rhodophyta), from Krabi, Thailand. – *Journal of Applied Phycology* 27: 1235-1242. <https://doi.org/10.1007/s10811-014-0409-0>.
- [22] Gao, K., Beardall, J., Häder, D.-P., Hall-Spencer, J. M., Gao, G., Hutchins, D. A. (2019): Effects of ocean acidification on marine photosynthetic organisms under the concurrent influences of warming, UV radiation, and deoxygenation. – *Frontiers in Marine Science* 6: 322. DOI: 10.3389/fmars.2019.00322.
- [23] George, R., Gullström, M., Mangora, M. M., Mtolera, M. S. P., Björk, M. (2018): High midday temperature stress has stronger effects on biomass than on photosynthesis: a mesocosm experiment on four tropical seagrass species. – *Ecology and Evolution* 8(9): 4508-4517. DOI: 10.1002/ece3.3952.
- [24] Gouvêa, L. P., Schubert, N., Martins, C. D. L., Sissini, M., Ramlov, F., Rodrigues, E. R. de O., Bastos, E. O., Freire, V. C., Maraschin, M., Simonassi, J. C., Varela, D. A., Franco, D., Cassano, V., Fonseca, A. L., Barufi, J. B., Horta, P. A. (2017): Interactive effects of marine heatwaves and eutrophication on the ecophysiology of a widespread and ecologically important macroalga. – *Limnology and Oceanography* 62(5): 2056-2075. DOI: 10.1002/lno.10551.
- [25] Graba-Landry, A., Hoey, A. S., Matley, J. K., Sheppard-Brennand, H., Poore, A. G. B., Byrne, M., Dworjanyn, S. A. (2018): Ocean warming has greater and more consistent negative effects than ocean acidification on the growth and health of subtropical macroalgae. – *Marine Ecology Progress Series* 595: 55-69. DOI: 10.3354/meps12552.
- [26] Harker, M., Berkaloff, C., Lemoine, Y., Britton, G., Young, A., Duval, J.-C., Rmiki, N.-E., Rousseau, B. (1999): Effects of high light and desiccation on the operation of the xanthophyll cycle in two marine brown algae. – *European Journal of Phycology* 34(1): 35-42. DOI: 10.1080/09670269910001736062.
- [27] Hill, R., Bellgrove, A., Macreadie, P. I., Petrou, K., Beardall, J., Steven, A., Ralph, P. J. (2015): Can macroalgae contribute to blue carbon? An Australian perspective. – *Limnology and Oceanography* 60(5): 1689-1706. DOI: 10.1002/lno.10128.
- [28] Ho, M., McBroom, J., Bergstrom, E., Diaz-Pulido, G. (2021): Physiological responses to temperature and ocean acidification in tropical fleshy macroalgae with varying affinities for inorganic carbon. – *ICES Journal of Marine Science* 78(1): 89-100. <https://doi.org/10.1093/icesjms/fsaa195>.
- [29] Hoegh-Guldberg, O., Jacob, D., Bindi, M., Brown, S., Camilloni, I., Diedhiou, A., Djalante, R., Ebi, K., Engelbrecht, F., Guiot, J. (2018): Chapter 3 Impacts of 1.5°C Global Warming on Natural and Human Systems. – In: *Global Warming of 1.5°C. An IPCC Special Report on the Impacts of Global Warming of 1.5°C above Pre-Industrial Levels and Related Global Greenhouse Gas Emission Pathways, in the Context of Strengthening the Global Response to the Threat of Climate Change, Sustainable Development, and Efforts to Eradicate Poverty*. IPCC, Geneva, pp.175-311.
- [30] Hofmann, L. C., Bischof, K. (2014): Ocean acidification effects on calcifying macroalgae. – *Aquatic Biology* 22: 261-279. DOI: 10.3354/ab00581.
- [31] Hurd, C. L., Harrison, P. J., Bischof, K., Lobban, C. S. (2014): *Seaweed Ecology and Physiology*. – Cambridge University Press, Cambridge.
- [32] Ihnken, S., Kromkamp, J. C., Beardall, J., Silsbe, G. M. (2014): State-transitions facilitate robust quantum yields and cause an over-estimation of electron transport in *Dunaliella tertiolecta* cells held at the CO₂ compensation point and re-supplied with DIC. – *Photosynthesis Research* 119: 257-272. <https://doi.org/10.1007/s11120-013-9937-8>.
- [33] Ji, Y., Xu, Z., Zou, D., Gao, K. (2016): Ecophysiological responses of marine macroalgae to climate change factors. – *Journal of Applied Phycology* 28: 2953-2967. <https://doi.org/10.1007/s10811-016-0840-5>.
- [34] Johnson, M. D., Carpenter, R. C. (2012): Ocean acidification and warming decrease calcification in the crustose coralline alga *Hydrolithon onkodes* and increase susceptibility to grazing. – *Journal of Experimental Marine Biology and Ecology* 434-435: 94-101. <https://doi.org/10.1016/j.jembe.2012.08.005>.

- [35] Johnson, M. D., Price, N. N., Smith, J. E. (2014): Contrasting effects of ocean acidification on tropical fleshy and calcareous algae. – *PeerJ* 2: 1-28. DOI: 10.7717/peerj.411.
- [36] Kalokora, O. J., Buriyo, A. S., Asplund, M. E., Gullström, M., Mtolera, M. S. P., Björk, M. (2020): An Experimental assessment of algal calcification as a potential source of atmospheric CO₂. – *PLoS One* 15(4): e0231971. DOI: 10.1371/journal.pone.0231971.
- [37] Kleypas, J. A., Buddemeier, R. W., Archer, D., Gattuso, J.-P., Langdon, C., Opdyke, B. N. (1999): Geochemical consequences of increased atmospheric carbon dioxide on coral reefs. – *Science* 284(5411): 118-120. DOI: 10.1126/science.284.5411.118.
- [38] Koch, M., Bowes, G., Ross, C., Zhang, X.-H. (2013): Climate change and ocean acidification effects on seagrasses and marine macroalgae. – *Global Change Biology* 19(1): 103-132. DOI: 10.1111/j.1365-2486.2012.02791.x.
- [39] König, K., Vaseghi, M. J., Dreyer, A., Dietz, K.-J. (2018): The significance of glutathione and ascorbate in modulating the retrograde high light response in *Arabidopsis thaliana* leaves. – *Physiologia Plantarum* 162(3): 262-273. DOI: 10.1111/ppl.12644.
- [40] Kram, S. L., Price, N. N., Donham, E. M., Johnson, M. D., Kelly, E. L. A., Hamilton, S. L., Smith, J. E. (2016): Variable responses of temperate calcified and fleshy macroalgae to elevated pCO₂ and warming. – *ICES Journal of Marine Science* 73(3): 693-703. DOI: 10.1093/icesjms/fsv168.
- [41] Kumar, Y. N., Poong, S.-W., Gachon, C., Brodie, J., Sade, A., Lim, P.-E. (2020): Impact of elevated temperature on the physiological and biochemical responses of *Kappaphycus alvarezii* (Rhodophyta). – *PLoS One* 15(9): e0239097. DOI: 10.1371/journal.pone.0239097.
- [42] Marques, J. A., Flores, F., Patel, F., Bianchini, A., Uthicke, S., Negri, A. P. (2020): Acclimation history modulates effect size of calcareous algae (*Halimeda opuntia*) to herbicide exposure under future climate scenarios. – *Science of the Total Environment* 739: 140308. DOI: 10.1016/j.scitotenv.2020.140308.
- [43] McDowell, R. E., Amsler, C. D., McClintock, J. B., Baker, B. J. (2014): Reactive oxygen species as a marine grazing defense: H₂O₂ and wounded *Ascoseira mirabilis* both inhibit feeding by an amphipod grazer. – *Journal of Experimental Marine Biology and Ecology* 458: 34-38. <https://doi.org/10.1016/j.jembe.2014.04.012>.
- [44] McNicholl, C., Koch, M. S. (2021): Irradiance, photosynthesis and elevated pCO₂ effects on net calcification in tropical reef macroalgae. – *Journal of Experimental Marine Biology and Ecology* 535: 151489. DOI: 10.1016/j.jembe.2020.151489.
- [45] McNicholl, C., Koch, M. S., Hofmann, L. C. (2019): Photosynthesis and light-dependent proton pumps increase boundary layer pH in tropical macroalgae: a proposed mechanism to sustain calcification under ocean acidification. – *Journal of Experimental Marine Biology and Ecology* 521: 151208. DOI: 10.1016/j.jembe.2019.151208.
- [46] McNicholl, C., Koch, M. S., Swarzenski, P. W., Oberhaensli, F. R., Taylor, A., Batista, M. G., Metian, M. (2020): Ocean acidification effects on calcification and dissolution in tropical reef macroalgae. – *Coral Reefs* 39: 1635-1647. DOI: 10.1007/s00338-020-01991-x.
- [47] Munoz, P. T., Saez, C. A., Martínez-Callejas, M. B., Flores-Molina, M. R., Bastos, E., Fonseca, A., Gurgel, C. F. D., Barufi, J. B., Roerig, L., Hall-Spencer, J. M. (2018): Short-term interactive effects of increased temperatures and acidification on the calcifying macroalgae *Lithothamnion crispatum* and *Sonderophycus capensis*. – *Aquatic Botany* 148: 46-52. <https://doi.org/10.1016/j.aquabot.2018.04.008>.
- [48] Nualla-ong, A., Phongdara, A., Buapet, P. (2020): Copper and zinc differentially affect root glutathione accumulation and phytochelatin synthase gene expression of *Rhizophora mucronata* seedlings: implications for mechanisms underlying trace metal tolerance. – *Ecotoxicology and Environmental Safty* 205: 111175. DOI: 10.1016/j.ecoenv.2020.111175.

- [49] Oakley, C. A., Schmidt, G. W., Hopkinson, B. M. (2014): Thermal responses of Symbiodinium photosynthetic carbon assimilation. – *Coral Reefs* 33: 501-512. <https://doi.org/10.1007/s00338-014-1130-9>.
- [50] Okazaki, M., Pentecost, A., Tanaka, Y., Miyata, M. (1986): A study of calcium carbonate deposition in the genus *Padina* (Phaeophyceae, Dictyotales). – *British Phycological Journal* 21(2): 217-224. DOI: 10.1080/00071618600650251.
- [51] Peach, K. E., Koch, M. S., Blackwelder, P. L. (2016): Effects of elevated $p\text{CO}_2$ and irradiance on growth, photosynthesis and calcification in *Halimeda discoidea*. – *Marine Ecology Progress Series* 544: 143-158. <https://doi.org/10.3354/meps11591>.
- [52] Pedersen, O., Colmer, T. D., Borum, J., Zavala-Perez, A., Kendrick, G. A. (2016): Heat stress of two tropical seagrass species during low tides-impact on underwater net photosynthesis, dark respiration and diel in situ internal aeration. – *New Phytologist* 210(4): 1207-1218. <https://doi.org/10.1111/nph.13900>.
- [53] Phandee, S., Hwan-air, W., Soonthornkalump, S., Jenke, M., Buapet, P. (2022): Experimental flooding modifies rhizosphere conditions, induces photoacclimation and promotes antioxidant activities in *Rhizophora mucronata* seedlings. – *Botanica Marina* 65: 1. <https://doi.org/10.1515/bot-2021-0051>.
- [54] Pierrot, D., Lewie, E., Wallace, D. W. R. (2006): MS Excel Program Developed for CO_2 System Calculations: ORNL/CDIAC-105a. – Carbon Dioxide Information Analysis Center, Oak Ridge National Laboratory, U.S. Department of Energy, Oak Ridge, Tennessee.
- [55] Platt, T., Gallegos, C. L., Harrison, W. G. (1980): Photoinhibition of photosynthesis in natural assemblages of marine phytoplankton. – *Journal of Marine Research* 38: 104-111.
- [56] Pörtner, H.-O., Roberts, D. C., Masson-Delmotte, V., Zhai, P., Tignor, M., Poloczanska, E., Weyer, N. M. (2019): The ocean and cryosphere in a changing climate. – IPCC Special Report on the Ocean and Cryosphere in a Changing Climate. IPCC, Geneva.
- [57] Prathep, A., Kaewsrihraw, R., Mayakun, J., Darakrai, A. (2018): The effects of light intensity and temperature on the calcification rate of *Halimeda Macroloba*. – *Journal of Applied Phycology* 30: 3405-3412. DOI: 10.1007/s10811-018-1534-y.
- [58] Price, N., Hamilton, S., Tootell, J., Smith, J. (2011): Species-specific consequences of ocean acidification for the calcareous tropical green algae *Halimeda*. – *Marine Ecology Progress Series* 440: 67-78. DOI: 10.3354/meps09309.
- [59] Ralph, P. J. (1999): Photosynthetic response of *Halophila ovalis* (R. Br.) Hook. f. to combined environmental stress. – *Aquatic Botany* 65(1-4): 83-96. [https://doi.org/10.1016/S0304-3770\(99\)00033-9](https://doi.org/10.1016/S0304-3770(99)00033-9).
- [60] Ralph, P. J., Gademann, R. (2005): Rapid light curves: a powerful tool to assess photosynthetic activity. – *Aquatic Botany* 82(3): 222-237. DOI: 10.1016/j.aquabot.2005.02.006.
- [61] Rasmusson, L. M., Buapet, P., George, R., Gullström, M., Gunnarsson, P. C. B., Björk, M. (2020): Effects of temperature and hypoxia on respiration, photorespiration, and photosynthesis of seagrass leaves from contrasting temperature regimes. – *ICES Journal of Marine Science* 77(6): 2056-2065. DOI: 10.1093/icesjms/fsaa093.
- [62] Rees, S. A., Opdyke, B. N., Wilson, P. A., Henstock, T. J. (2007): Significance of *Halimeda* bioherms to the global carbonate budget based on a geological sediment budget for the northern great barrier reef, Australia. – *Coral Reefs* 26: 177-188. DOI: 10.1007/s00338-006-0166-x.
- [63] Román, M., Román, S., Vázquez, E., Troncoso, J., Olabarria, C. (2020): Heatwaves during low tide are critical for the physiological performance of intertidal macroalgae under global warming scenarios. – *Scientific Reports* 10: 21408. DOI: 10.1038/s41598-020-78526-5.
- [64] Ross, C. L., Warnes, A., Comeau, S., Cornwall, C. E., Cuttler, M. V. W., Naugle, M., McCulloch, M. T., Schoepf, V. (2022): Coral calcification mechanisms in a warming ocean and the interactive effects of temperature and light. – *Communications Earth & Environment* 3: 72. <https://doi.org/10.1038/s43247-022-00396-8>.

- [65] Saewong, C., Namnapol, S., Ng, M. S., Sinutok, S., Buapet, P. (2021): Effects of warming on carbon utilization and photosynthesis of marine primary producers. – *Journal of Fisheries and Environment* 45(3): 89-99.
- [66] Saewong, C., Soonthornkalump, S., Buapet, P. (2022): Combined effects of high irradiance and temperature on the photosynthetic and antioxidant responses of *Thalassia hemprichii* and *Halophila ovalis*. – *Botanica Marina* 65(5). DOI: 10.1515/bot-2022-0014.
- [67] Sainz, M., Díaz, P., Monza, J., Borsani, O. (2010): Heat stress results in loss of chloroplast Cu/Zn superoxide dismutase and increased damage to photosystem II in combined drought-heat stressed *Lotus Japonicus*. – *Physiologia Plantarum* 140(1): 46-56. DOI: 10.1111/j.1399-3054.2010.01383.x.
- [68] Scherner, F., Pereira, C. M., Duarte, G., Horta, P. A., e Castro, C. B., Barufi, J. B., Pereira, S. M. B. (2016): Effects of ocean acidification and temperature increases on the photosynthesis of tropical reef calcified macroalgae. – *PLoS One* 11(5): e0154844. DOI: 10.1371/journal.pone.0154844.
- [69] Schubert, N., Hofmann, L. C., Almeida Saá, A. C., Moreira, A. C., Arenhart, R. G., Fernandes, C. P., de Beer, D., Horta, P. A., Silva, J. (2021): Calcification in free-living coralline algae is strongly influenced by morphology: implications for susceptibility to ocean acidification. – *Scientific Reports* 11(1): 11232. DOI: 10.1038/s41598-021-90632-6.
- [70] Shiu, C.-T., Lee, T.-M. (2005): Ultraviolet-B-induced oxidative stress and responses of the ascorbate–glutathione cycle in a marine macroalga *Ulva fasciata*. – *Journal of Experimental Botany* 56: 2851-2865. DOI: 10.1093/jxb/eri277.
- [71] Sinutok, S., Pongparadon, S., Prathep, A. (2008): Seasonal variation in density, growth rate and calcium carbonate accumulation of *Halimeda macroloba* Decaisne at Tangkhen Bay, Phuket Province, Thailand. – *Malaysian Journal of Science* 27(2): 1-8.
- [72] Sinutok, S., Hill, R., Doblin, M. A., Wuhler, R., Ralph, P. J. (2011): Warmer more acidic conditions cause decreased productivity and calcification in subtropical coral reef sediment-dwelling calcifiers. – *Limnology and Oceanography* 56(4): 1200-1212. DOI: 10.4319/lo.2011.56.4.1200.
- [73] Sinutok, S., Hill, R., Doblin, M. A., Kühl, M., Ralph, P. J. (2012): Microenvironmental changes support evidence of photosynthesis and calcification inhibition in *Halimeda* under ocean acidification and warming. – *Coral Reefs* 31: 1201-1213. DOI: 10.1007/s00338-012-0952-6.
- [74] Tait, L. W., Schiel, D. R. (2013): Impacts of temperature on primary productivity and respiration in naturally structured macroalgal assemblages. – *PLoS One* 8(9): e74413. <https://doi.org/10.1371/journal.pone.0074413>.
- [75] Tanzil, J. T. I., Brown, B. E., Tudhope, A. W., Dunne, R. P. (2009): Decline in skeletal growth of the coral *Porites lutea* from the Andaman Sea, South Thailand between 1984 and 2005. – *Coral Reefs* 28: 519-528. DOI: 10.1007/s00338-008-0457-5.
- [76] Wei, Z., Mo, J., Huang, R., Hu, Q., Long, C., Ding, D., Yang, F., Long, L. (2020): Physiological performance of three calcifying green macroalgae *Halimeda* species in response to altered seawater temperatures. – *Acta Oceanologica Sinica* 39: 89-100. DOI: 10.1007/s13131-019-1471-3.
- [77] Yang, F., Wei, Z., Long, L. (2021): Transcriptomic and physiological responses of the tropical reef calcified macroalga *Amphiroa fragilissima* to elevated temperature¹. – *Journal Phycology* 57(4): 1254-1265. DOI: 10.1111/jpy.13158.
- [78] Yucharoen, M., Sinutok, S., Chotikarn, P., Buapet, P. (2021): Experimental assessment of vulnerability to warming in tropical shallow-water marine organisms. – *Frontiers in Marine Science* 8: 767628. DOI: 10.3389/fmars.2021.767628.
- [79] Zuñiga-Rios, D., Vásquez-Elizondo, R. M., Caamal, E., Robledo, D. (2021): Photosynthetic responses of *Halimeda scabra* (Chlorophyta, Bryopsidales) to interactive effects of temperature, pH, and nutrients and its carbon pathways. – *PeerJ* 9: e10958. DOI: 10.7717/peerj.10958.

APPENDIX

Table A1. Summary of repeated ANOVAs of pH for *Halimeda macroloba* in responses to temperature, light, and time treatments. Significant values ($p < 0.05$) are shown in bold

	Effect	SS	df	MS	F	p
Time1	Intercept	5588.795	1	5588.795	880133.0	0.000000
	Temperature	0.011	2	0.006	0.9	0.415643
	Light	0.000	1	0.000	0.0	0.923443
	Temperature*Light	0.011	2	0.005	0.9	0.434841
	Error	0.222	35	0.006		
	Time	0.377	1	0.377	43.2	0.000000
	Time*Temperature	0.011	2	0.005	0.6	0.543364
	Time*Light	0.000	1	0.000	0.0	0.957929
	Time*Temperature*Light	0.005	2	0.003	0.3	0.745231
	Error	0.305	35	0.009		
Time2	Intercept	4985.122	1	4985.122	363769.4	0.000000
	Temperature	0.067	2	0.033	2.4	0.105473
	Light	0.050	1	0.050	3.6	0.066264
	Temperature*Light	0.069	2	0.034	2.5	0.098089
	Error	0.411	30	0.014		
	Time	0.660	1	0.660	36.4	0.000001
	Time*Temperature	0.111	2	0.055	3.1	0.061636
	Time*Light	0.050	1	0.050	2.7	0.107801
	Time*Temperature*Light	0.069	2	0.034	1.9	0.167219
	Error	0.544	30	0.018		
Time3	Intercept	4963.843	1	4963.843	1979574.2	0.000000
	Temperature	0.114	2	0.057	22.7	0.000001
	Light	0.012	1	0.012	4.9	0.034704
	Temperature*Light	0.054	2	0.027	10.8	0.000291
	Error	0.075	30	0.003		
	Time	0.446	1	0.446	91.3	0.000000
	Time*Temperature	0.125	2	0.062	12.8	0.000097
	Time*Light	0.012	1	0.012	2.5	0.123473
	Time*Temperature*Light	0.054	2	0.027	5.5	0.008899
	Error	0.147	30	0.005		

Table A2. Summary of repeated ANOVAs of pH for *Halimeda opuntia* in responses to temperature, light, and time treatments. Significant values ($p < 0.05$) are shown in bold

	Effect	SS	df	MS	F	p
Time1	Intercept	5714.665	1	5714.665	891942.5	0.000000
	Temperature	0.047	2	0.023	3.7	0.035684
	Light	0.000	1	0.000	0.0	0.885207
	Temperature*Light	0.005	2	0.003	0.4	0.665162
	Error	0.231	36	0.006		
	Time	0.284	1	0.284	47.7	0.000000
	Time*Temperature	0.030	2	0.015	2.5	0.093884
	Time*Light	0.000	1	0.000	0.0	0.826007
	Time*Temperature*Light	0.005	2	0.003	0.4	0.653842
	Error	0.215	36	0.006		
Time2	Intercept	4957.092	1	4957.092	2151331.4	0.000000
	Temperature	0.047	2	0.023	10.1	0.000440
	Light	0.004	1	0.004	1.9	0.174385
	Temperature*Light	0.027	2	0.014	5.9	0.006809
	Error	0.069	30	0.002		
	Time	0.337	1	0.337	55.8	0.000000
	Time*Temperature	0.074	2	0.037	6.1	0.005814
	Time*Light	0.004	1	0.004	0.7	0.397039
	Time*Temperature*Light	0.027	2	0.014	2.3	0.122063
	Error	0.181	30	0.006		
Time3	Intercept	4961.851	1	4961.851	3387785.4	0.000000
	Temperature	0.091	2	0.046	31.1	0.000000
	Light	0.009	1	0.009	6.4	0.017085
	Temperature*Light	0.059	2	0.029	20.1	0.000003
	Error	0.044	30	0.001		
	Time	0.413	1	0.413	98.2	0.000000
	Time*Temperature	0.076	2	0.038	9.0	0.000876
	Time*Light	0.009	1	0.009	2.2	0.146737
	Time*Temperature*Light	0.059	2	0.029	7.0	0.003204
	Error	0.126	30	0.004		

Table A3. Summary of repeated ANOVAs of pH for *Padina boryana* in responses to temperature, light, and time treatments. Significant values ($p < 0.05$) are shown in bold

	Effect	SS	df	MS	F	p
Time1	Intercept	4922.718	1	4922.718	173708.3	0.000000
	Temperature	0.375	2	0.188	6.6	0.004160
	Light	0.037	1	0.037	1.3	0.263328
	Temperature*Light	0.031	2	0.016	0.6	0.580733
	Error	0.850	30	0.028		
	Time	0.621	1	0.621	48.5	0.000000
	Time*Temperature	0.268	2	0.134	10.5	0.000352
	Time*Light	0.034	1	0.034	2.6	0.115583
	Time*Temperature*Light	0.033	2	0.016	1.3	0.293314
	Error	0.384	30	0.013		
Time2	Intercept	4158.058	1	4158.058	230698.4	0.000000
	Temperature	0.223	2	0.112	6.2	0.006792
	Light	0.020	1	0.020	1.1	0.305353
	Temperature*Light	0.045	2	0.022	1.2	0.306125
	Error	0.433	24	0.018		
	Time	0.531	1	0.531	26.9	0.000026
	Time*Temperature	0.403	2	0.202	10.2	0.000620
	Time*Light	0.020	1	0.020	1.0	0.327035
	Time*Temperature*Light	0.045	2	0.022	1.1	0.337987
	Error	0.474	24	0.020		
Time3	Intercept	4208.940	1	4208.940	139061.5	0.000000
	Temperature	0.834	2	0.417	13.8	0.000104
	Light	0.096	1	0.096	3.2	0.087169
	Temperature*Light	0.167	2	0.084	2.8	0.083294
	Error	0.726	24	0.030		
	Time	1.345	1	1.345	42.5	0.000001
	Time*Temperature	0.732	2	0.366	11.6	0.000303
	Time*Light	0.096	1	0.096	3.0	0.093982
	Time*Temperature*Light	0.167	2	0.084	2.6	0.091955
	Error	0.760	24	0.032		

Table A4. Summary of repeated ANOVAs of total alkalinity for *Halimeda macroloba* in responses to temperature, light, and time treatments. Significant values ($p < 0.05$) are shown in bold

	Effect	SS	df	MS	F	p
Time1	Intercept	355909728	1	355909728	7219.4	0.000000
	Temperature	4178676	2	2089338	42.4	0.000000
	Light	31656	1	31656	0.6	0.428197
	Temperature*Light	5923	2	2961	0.1	0.941792
	Error	1774760	36	49299		
	Time	421222	1	421222	18.0	0.000145
	Time*Temperature	2812503	2	1406252	60.2	0.000000
	Time*Light	58620	1	58620	2.5	0.121792
	Time*Temperature*Light	5024	2	2512	0.1	0.898270
	Error	840396	36	23344		
Time2	Intercept	331981563	1	331981563	4728.4	0.000000
	Temperature	2767069	2	1383534	19.7	0.000002
	Light	14598	1	14598	0.2	0.651143
	Temperature*Light	28909	2	14455	0.2	0.814885
	Error	2527588	36	70211		
	Time	756210	1	756210	39.4	0.000000
	Time*Temperature	2563098	2	1281549	66.7	0.000000
	Time*Light	14598	1	14598	0.8	0.389221
	Time*Temperature*Light	28909	2	14455	0.8	0.478606
	Error	691828	36	19217		
Time3	Intercept	340685763	1	340685763	6923.4	0.000000
	Temperature	2009800	2	1004900	20.4	0.000001
	Light	1168	1	1168	0.0	0.878398
	Temperature*Light	19736	2	9868	0.2	0.819200
	Error	1771494	36	49208		
	Time	480663	1	480663	31.4	0.000002
	Time*Temperature	1697883	2	848942	55.4	0.000000
	Time*Light	1168	1	1168	0.1	0.783973
	Time*Temperature*Light	19736	2	9868	0.6	0.530979
	Error	551374	36	15316		

Table A5. Summary of repeated ANOVAs of total alkalinity of *Halimeda opuntia* in responses to temperature, light, and time treatments. Significant values ($p < 0.05$) are shown in bold

	Effect	SS	df	MS	F	p
Time1	Intercept	343812422	1	343812422	8681.2	0.000000
	Temperature	3870879	2	1935440	48.9	0.000000
	Light	25099	1	25099	0.6	0.431206
	Temperature*Light	176795	2	88397	2.2	0.121956
	Error	1425758	36	39604		
	Time	273509	1	273509	9.1	0.004693
	Time*Temperature	2760988	2	1380494	45.9	0.000000
	Time*Light	33778	1	33778	1.1	0.296458
	Time*Temperature*Light	174211	2	87105	2.9	0.068290
	Error	1083394	36	30094		
Time2	Intercept	341438727	1	341438727	9662.2	0.000000
	Temperature	3095396	2	1547698	43.8	0.000000
	Light	6326	1	6326	0.2	0.674733
	Temperature*Light	114026	2	57013	1.6	0.213284
	Error	1272152	36	35338		
	Time	637421	1	637421	35.7	0.000001
	Time*Temperature	2337076	2	1168538	65.4	0.000000
	Time*Light	6326	1	6326	0.4	0.555523
	Time*Temperature*Light	114026	2	57013	3.2	0.052976
	Error	643155	36	17865		
Time3	Intercept	333631179	1	333631179	10994.3	0.000000
	Temperature	1727973	2	863986	28.5	0.000000
	Light	1543	1	1543	0.1	0.822890
	Temperature*Light	148736	2	74368	2.5	0.100500
	Error	1092455	36	30346		
	Time	892650	1	892650	49.5	0.000000
	Time*Temperature	1658259	2	829129	46.0	0.000000
	Time*Light	1543	1	1543	0.1	0.771506
	Time*Temperature*Light	148736	2	74368	4.1	0.024332
	Error	648663	36	18018		

Table A6. Summary of repeated ANOVAs of total alkalinity (TA) for *Padina boryana* in responses to temperature, light, and time treatments. Significant values ($p < 0.05$) are shown in bold

	Effect	SS	df	MS	F	p
Time1	Intercept	296775526	1	296775526	9846.0	0.000000
	Temperature	317645	2	158823	5.3	0.010935
	Light	27526	1	27526	0.9	0.346900
	Temperature*Light	31790	2	15895	0.5	0.595537
	Error	904252	30	30142		
	Time	569978	1	569978	47.1	0.000000
	Time*Temperature	164690	2	82345	6.8	0.003658
	Time*Light	7974	1	7974	0.7	0.423334
	Time*Temperature*Light	11077	2	5538	0.5	0.637127
	Error	363067	30	12102		
Time2	Intercept	290636978	1	290636978	7099.9	0.000000
	Temperature	333492	2	166746	4.1	0.027224
	Light	12405	1	12405	0.3	0.586062
	Temperature*Light	32978	2	16489	0.4	0.672005
	Error	1228068	30	40936		
	Time	511125	1	511125	33.6	0.000002
	Time*Temperature	246801	2	123400	8.1	0.001531
	Time*Light	12405	1	12405	0.8	0.373831
	Time*Temperature*Light	32978	2	16489	1.1	0.351334
	Error	456610	30	15220		
Time3	Intercept	294923416	1	294923416	20935.4	0.000000
	Temperature	128580	2	64290	4.6	0.018604
	Light	3363	1	3363	0.2	0.628685
	Temperature*Light	5790	2	2895	0.2	0.815375
	Error	422619	30	14087		
	Time	453046	1	453046	62.1	0.000000
	Time*Temperature	162410	2	81205	11.1	0.000242
	Time*Light	4706	1	4706	0.6	0.428162
	Time*Temperature*Light	3818	2	1909	0.3	0.771435
	Error	218805	30	7294		

Table A7. Summary of repeated ANOVAs of dissolved inorganic carbon (DIC) uptake for *Halimeda macroloba*, *Halimeda opuntia*, and *Padina boryana* in responses to temperature, light, and time treatments. Significant values ($p < 0.05$) are shown in bold

	Effect	SS	df	MS	F	p
<i>Halimeda macroloba</i>	Intercept	3015.714	1	3015.714	87.70288	0.000000
	Temperature	2049.413	2	1024.706	29.80047	0.000000
	Light	50.995	1	50.995	1.48304	0.231221
	Temperature*Light	130.104	2	65.052	1.89184	0.165484
	Error	1237.881	36	34.386		
	Time	57.765	2	28.882	3.28420	0.043156
	Time*Temperature	131.955	4	32.989	3.75113	0.007912
	Time*Light	16.079	2	8.040	0.91419	0.405443
	Time*Temperature*Light	28.845	4	7.211	0.81998	0.516656
	Error	633.191	72	8.794		
<i>Halimeda opuntia</i>	Intercept	2712.525	1	2712.525	58.41829	0.000000
	Temperature	2280.563	2	1140.282	24.55767	0.000000
	Light	13.508	1	13.508	0.29092	0.592951
	Temperature*Light	547.100	2	273.550	5.89131	0.006118
	Error	1671.581	36	46.433		
	Time	100.295	2	50.147	3.67412	0.030243
	Time*Temperature	42.200	4	10.550	0.77296	0.546363
	Time*Light	10.024	2	5.012	0.36722	0.693944
	Time*Temperature*Light	82.864	4	20.716	1.51779	0.206080
	Error	982.715	72	13.649		
<i>Padina boryana</i>	Intercept	3856.482	1	3856.482	82.81686	0.000000
	Temperature	2198.540	2	1099.270	23.60651	0.000001
	Light	120.720	1	120.720	2.59242	0.117850
	Temperature*Light	226.027	2	113.014	2.42694	0.105452
	Error	1396.992	30	46.566		
	Time	97.472	2	48.736	5.87765	0.004666
	Time*Temperature	64.358	4	16.089	1.94042	0.115355
	Time*Light	4.931	2	2.466	0.29735	0.743876
	Time*Temperature*Light	18.694	4	4.674	0.56364	0.689939
	Error	497.505	60	8.292		

Table A8. Summary of repeated ANOVAs of calcification rate for *Halimeda macroloba*, *Halimeda opuntia*, and *Padina boryana* in responses to temperature, light, and time treatments. Significant values ($p < 0.05$) are shown in bold

	Effect	SS	df	MS	F	p
<i>Halimeda macroloba</i>	Intercept	715.366	1	715.366	39.29964	0.000000
	Temperature	3151.418	2	1575.709	86.56374	0.000000
	Light	16.511	1	16.511	0.90704	0.347252
	Temperature*Light	26.002	2	13.001	0.71422	0.496380
	Error	655.304	36	18.203		
	Time	25.299	2	12.649	3.61039	0.032045
	Time*Temperature	198.998	4	49.749	14.19954	0.000000
	Time*Light	3.632	2	1.816	0.51829	0.597742
	Time*Temperature*Light	8.435	4	2.109	0.60185	0.662516
	Error	252.259	72	3.504		
<i>Halimeda opuntia</i>	Intercept	837.618	1	837.618	38.63699	0.000000
	Temperature	3698.191	2	1849.096	85.29369	0.000000
	Light	19.888	1	19.888	0.91738	0.344553
	Temperature*Light	10.715	2	5.357	0.24712	0.782364
	Error	780.450	36	21.679		
	Time	21.435	2	10.718	2.50483	0.088786
	Time*Temperature	253.762	4	63.441	14.82665	0.000000
	Time*Light	9.939	2	4.969	1.16137	0.318853
	Time*Temperature*Light	11.326	4	2.832	0.66176	0.620584
	Error	308.075	72	4.279		
<i>Padina boryana</i>	Intercept	844.125	1	844.125	100.87066	0.000000
	Temperature	321.090	2	160.545	19.18472	0.000004
	Light	2.750	1	2.750	0.32865	0.570726
	Temperature*Light	13.552	2	6.776	0.80972	0.454470
	Error	251.052	30	8.368		
	Time	6.251	2	3.125	0.83985	0.436787
	Time*Temperature	4.316	4	1.079	0.28992	0.883407
	Time*Light	8.723	2	4.362	1.17200	0.316735
	Time*Temperature*Light	8.380	4	2.095	0.56298	0.690413
	Error	223.285	60	3.721		

Table A9. Summary of repeated ANOVAs of effective quantum yield (EQY) for *Halimeda macroloba*, *Halimeda opuntia*, and *Padina boryana* in responses to temperature, light, and time treatments. Significant values ($p < 0.05$) are shown in bold

	Effect	SS	df	MS	F	p
<i>Halimeda macroloba</i>	Intercept	1.423915	1	1.423915	595.8972	0.000000
	Temperature	0.418706	2	0.209353	87.6126	0.000000
	Light	0.598769	1	0.598769	250.5800	0.000000
	Temperature*Light	0.378021	2	0.189011	79.0994	0.000000
	Error	0.071686	30	0.002390		
	Time	0.000602	2	0.000301	0.7987	0.454620
	Time*Temperature	0.002555	4	0.000639	1.6944	0.163130
	Time*Light	0.000319	2	0.000160	0.4235	0.656705
	Time*Temperature*Light	0.001412	4	0.000353	0.9364	0.449112
	Error	0.022623	60	0.000377		
<i>Halimeda opuntia</i>	Intercept	1.332629	1	1.332629	2650.5792	0.000000
	Temperature	0.308599	2	0.154300	306.8996	0.000000
	Light	0.528033	1	0.528033	1050.2497	0.000000
	Temperature*Light	0.293711	2	0.146855	292.0931	0.000000
	Error	0.015083	30	0.000503		
	Time	0.000375	2	0.000188	0.4621	0.632199
	Time*Temperature	0.003182	4	0.000795	1.9593	0.112300
	Time*Light	0.000223	2	0.000111	0.2746	0.760819
	Time*Temperature*Light	0.001574	4	0.000394	0.9695	0.430944
	Error	0.024358	60	0.000406		
<i>Padina boryana</i>	Intercept	5.832767	1	5.832767	531.8727	0.000000
	Temperature	0.074498	2	0.037249	3.3966	0.046805
	Light	0.550813	1	0.550813	50.2270	0.000000
	Temperature*Light	0.176726	2	0.088363	8.0576	0.001582
	Error	0.328994	30	0.010966		
	Time	0.037292	2	0.018646	2.7960	0.069028
	Time*Temperature	0.044348	4	0.011087	1.6625	0.170560
	Time*Light	0.215806	2	0.107903	16.1798	0.000002
	Time*Temperature*Light	0.019173	4	0.004793	0.7187	0.582484
	Error	0.400139	60	0.006669		

Table A10. Summary of repeated ANOVAs of maximum quantum yield (MQY) for *Halimeda macroloba*, *Halimeda opuntia*, and *Padina boryana* in responses to temperature, light, and time treatments. Significant values ($p < 0.05$) are shown in bold

	Effect	SS	df	MS	F	p
<i>Halimeda macroloba</i>	Intercept	25.51113	1	25.51113	14481.36	0.000000
	Temperature	1.45469	2	0.72734	412.88	0.000000
	Light	0.03404	1	0.03404	19.32	0.000127
	Temperature*Light	0.01719	2	0.00859	4.88	0.014641
	Error	0.05285	30	0.00176		
	Time	2.40358	1	2.40358	1650.32	0.000000
	Time*Temperature	1.33214	2	0.66607	457.33	0.000000
	Time*Light	0.05120	1	0.05120	35.15	0.000002
	Time*Temperature*Light	0.03264	2	0.01632	11.21	0.000232
	Error	0.04369	30	0.00146		
<i>Halimeda opuntia</i>	Intercept	26.48860	1	26.48860	15133.04	0.000000
	Temperature	1.36548	2	0.68274	390.05	0.000000
	Light	0.00740	1	0.00740	4.23	0.048502
	Temperature*Light	0.00951	2	0.00476	2.72	0.082344
	Error	0.05251	30	0.00175		
	Time	1.87241	1	1.87241	1194.16	0.000000
	Time*Temperature	1.40751	2	0.70375	448.83	0.000000
	Time*Light	0.01191	1	0.01191	7.59	0.009863
	Time*Temperature*Light	0.00942	2	0.00471	3.00	0.064650
	Error	0.04704	30	0.00157		
<i>Padina boryana</i>	Intercept	29.29373	1	29.29373	8764.87	0.000000
	Temperature	0.56962	2	0.28481	85.22	0.000000
	Light	0.01469	1	0.01469	4.39	0.044600
	Temperature*Light	0.00122	2	0.00061	0.18	0.833651
	Error	0.10027	30	0.00334		
	Time	0.67545	1	0.67545	213.59	0.000000
	Time*Temperature	0.58190	2	0.29095	92.00	0.000000
	Time*Light	0.01576	1	0.01576	4.98	0.033219
	Time*Temperature*Light	0.00158	2	0.00079	0.25	0.780220
	Error	0.09487	30	0.00316		

Table A11. Summary of univariate test of significance for maximum electron transport rate (ETR_{max}) of *Halimeda macroloba*, *Halimeda opuntia*, and *Padina boryana* in responses to temperature and light treatments. Significant values ($p < 0.05$) are shown in bold

	Effect	SS	df	MS	F	p
<i>Halimeda macroloba</i>	Intercept	2374.450	1	2374.450	312.6336	0.000000
	Temperature	453.851	2	226.925	29.8783	0.000022
	Light	92.998	1	92.998	12.2446	0.004388
	Temperature*Light	164.706	2	82.353	10.8431	0.002044
	Error	91.140	12	7.595		
<i>Halimeda opuntia</i>	Intercept	3020.304	1	3020.304	92.72285	0.000001
	Temperature	308.669	2	154.335	4.73805	0.030434
	Light	142.910	1	142.910	4.38732	0.058100
	Temperature*Light	47.583	2	23.791	0.73039	0.501954
	Error	390.882	12	32.573		
<i>Padina boryana</i>	Intercept	26197.48	1	26197.48	96.13962	0.000000
	Temperature	3155.87	2	1577.93	5.79070	0.017365
	Light	0.17	1	0.17	0.00064	0.980244
	Temperature*Light	425.67	2	212.84	0.78107	0.479865
	Error	3269.93	12	272.49		

Table A12. Summary of univariate test of significance for saturating irradiance (E_k) of *Halimeda macroloba*, *Halimeda opuntia*, and *Padina boryana* in responses to temperature and light treatments. Significant values ($p < 0.05$) are shown in bold

	Effect	SS	df	MS	F	p
<i>Halimeda macroloba</i>	Intercept	767807.1	1	767807.1	16.30545	0.001645
	Temperature	347791.2	2	173895.6	3.69292	0.056258
	Light	33.4	1	33.4	0.00071	0.979205
	Temperature*Light	219289.4	2	109644.7	2.32846	0.139804
	Error	565067.8	12	47089.0		
<i>Halimeda opuntia</i>	Intercept	395982.1	1	395982.1	86.51004	0.000001
	Temperature	89583.5	2	44791.8	9.78563	0.003015
	Light	29753.1	1	29753.1	6.50015	0.025487
	Temperature*Light	13809.3	2	6904.7	1.50846	0.260377
	Error	54927.6	12	4577.3		
<i>Padina boryana</i>	Intercept	843351.3	1	843351.3	155.9199	0.000000
	Temperature	1198.0	2	599.0	0.1107	0.896073
	Light	11769.3	1	11769.3	2.1759	0.165934
	Temperature*Light	21684.4	2	10842.2	2.0045	0.177376
	Error	64906.5	12	5408.9		

Table A13. Summary of univariate test of significance for alpha of *Halimeda macroloba*, *Halimeda opuntia*, and *Padina boryana* in responses to temperature and light treatments. Significant values ($p < 0.05$) are shown in bold

	Effect	SS	df	MS	F	p
<i>Halimeda macroloba</i>	Intercept	0.406249	1	0.406249	638.5453	0.000000
	Temperature	0.243235	2	0.121618	191.1593	0.000000
	Light	0.022262	1	0.022262	34.9915	0.000071
	Temperature*Light	0.014207	2	0.007104	11.1654	0.001824
	Error	0.007635	12	0.000636		
<i>Halimeda opuntia</i>	Intercept	0.418796	1	0.418796	294.0815	0.000000
	Temperature	0.221748	2	0.110874	77.8566	0.000000
	Light	0.015413	1	0.015413	10.8231	0.006461
	Temperature*Light	0.011098	2	0.005549	3.8965	0.049662
	Error	0.017089	12	0.001424		
<i>Padina boryana</i>	Intercept	0.619273	1	0.619273	572.0228	0.000000
	Temperature	0.087913	2	0.043957	40.6026	0.000005
	Light	0.012283	1	0.012283	11.3455	0.005588
	Temperature*Light	0.005744	2	0.002872	2.6531	0.111145
	Error	0.012991	12	0.001083		

Table A14. Regression modeling of dissolved inorganic carbon uptake rate (x axis) and calcification rate (y axis) for *Halimeda macroloba*, *Halimeda opuntia*, and *Padina boryana*

Species	Hour	Intercept	Slope	p_value	Equation
<i>Halimeda macroloba</i>	1	-1.52	0.55	< 0.001	$y = -1.52 + 0.55x$
	2	-1.03	0.45	< 0.001	$y = -1.03 + 0.45x$
	3	-1.17	0.51	< 0.001	$y = -1.17 + 0.51x$
<i>Halimeda opuntia</i>	1	-0.64	0.51	< 0.001	$y = -0.64 + 0.51x$
	2	-0.42	0.48	< 0.001	$y = -0.42 + 0.48x$
	3	-1.32	0.44	< 0.001	$y = -1.32 + 0.44x$
<i>Padina boryana</i>	1	0.73	0.28	< 0.001	$y = 0.73 + 0.28x$
	2	0.16	0.33	< 0.001	$y = 0.16 + 0.33x$
	3	0.82	0.18	< 0.001	$y = 0.82 + 0.18x$

Table A15. Regression modeling of relative electron transport rate (rETR) (x axis) and calcification rate (y axis) for *Halimeda macroloba*, *Halimeda opuntia*, and *Padina boryana*

Species	Hour	Intercept	Slope	p_value	Equation
<i>Halimeda macroloba</i>	1	-4.81	0.21	< 0.001	$y = -4.81 + 0.21x$
	2	-2.71	0.16	< 0.001	$y = -2.71 + 0.16x$
	3	-0.57	0.08	0.067	$y = -0.57 + 0.08x$
<i>Halimeda opuntia</i>	1	-5.48	0.23	< 0.001	$y = -5.48 + 0.23x$
	2	-1.29	0.12	0.016	$y = -1.29 + 0.12x$
	3	0.7	0.05	0.307	$y = 0.7 + 0.05x$
<i>Padina boryana</i>	1	1.54	0.02	0.022	$y = 1.54 + 0.02x$
	2	2.5	0	0.848	$y = 2.5 + 0x$
	3	3.24	-0.01	0.279	$y = 3.24 + -0.01x$

Table A16. Summary of univariate tests of significance for reactive oxygen species (ROS) of *Halimeda macroloba*, *Halimeda opuntia*, and *Padina boryana* in responses to temperature and light treatments. Significant values ($p < 0.05$) are shown in bold

A. Reactive Oxygen Species (ROS)						
	Effect	SS	df	MS	F	p
<i>Halimeda macroloba</i>	Intercept	0.633460	1	0.633460	90.97119	0.000000
	Temperature	0.072509	2	0.036254	5.20648	0.010484
	Light	0.018807	1	0.018807	2.70086	0.109249
	Temperature*Light	0.002557	2	0.001278	0.18358	0.833079
	Error	0.243716	35	0.006963		
<i>Halimeda opuntia</i>	Intercept	71.21107	1	71.21107	69.25143	0.000000
	Temperature	33.48190	2	16.74095	16.28026	0.000009
	Light	2.50276	1	2.50276	2.43388	0.127487
	Temperature*Light	1.81913	2	0.90957	0.88454	0.421688
	Error	37.01871	36	1.02830		
<i>Padina boryana</i>	Intercept	0.258180	1	0.258180	78.46646	0.000000
	Temperature	0.059847	2	0.029923	9.09440	0.000780
	Light	0.013222	1	0.013222	4.01840	0.053808
	Temperature*Light	0.006388	2	0.003194	0.97077	0.390011
	Error	0.102000	31	0.003290		

Table A17. Summary of univariate tests of significance for Superoxide dismutase (SOD) of *Halimeda macroloba*, *Halimeda opuntia*, and *Padina boryana* in responses to temperature and light treatments. Significant values ($p < 0.05$) are shown in bold

B. Superoxide dismutase (SOD)						
	Effect	SS	df	MS	F	p
<i>Halimeda macroloba</i>	Intercept	24661.29	1	24661.29	221.9562	0.000000
	Temperature	1910.52	2	955.26	8.5975	0.000887
	Light	0.53	1	0.53	0.0048	0.945181
	Temperature*Light	147.86	2	73.93	0.6654	0.520277
	Error	3999.92	36	111.11		
<i>Halimeda opuntia</i>	Intercept	33816.47	1	33816.47	311.7633	0.000000
	Temperature	3507.05	2	1753.53	16.1662	0.000010
	Light	3.24	1	3.24	0.0298	0.863814
	Temperature*Light	251.44	2	125.72	1.1591	0.325217
	Error	3904.86	36	108.47		
<i>Padina boryana</i>	Intercept	1918.894	1	1918.894	29.22474	0.000004
	Temperature	63.302	2	31.651	0.48205	0.621446
	Light	0.991	1	0.991	0.01509	0.902929
	Temperature*Light	3.137	2	1.568	0.02389	0.976412
	Error	2363.757	36	65.660		

Table A18. Summary of univariate tests of significance for guaiacol peroxidase (GPOX) of *Halimeda macroloba*, *Halimeda opuntia*, and *Padina boryana* in responses to temperature and light treatments. Significant values ($p < 0.05$) are shown in bold

C. Guaiacol peroxidase (GPOX)						
	Effect	SS	df	MS	F	p
<i>Halimeda macroloba</i>	Intercept	967362.8	1	967362.8	436.8149	0.000000
	Temperature	9333.8	2	4666.9	2.1073	0.139197
	Light	346.4	1	346.4	0.1564	0.695267
	Temperature*Light	1973.8	2	986.9	0.4456	0.644587
	Error	66437.5	30	2214.6		
<i>Halimeda opuntia</i>	Intercept	1181215	1	1181215	411.2244	0.000000
	Temperature	17841	2	8921	3.1056	0.059454
	Light	3746	1	3746	1.3043	0.262471
	Temperature*Light	9488	2	4744	1.6515	0.208719
	Error	86173	30	2872		
<i>Padina boryana</i>	Intercept	1340181	1	1340181	465.2256	0.000000
	Temperature	20559	2	10280	3.5684	0.040713
	Light	7039	1	7039	2.4437	0.128490
	Temperature*Light	20339	2	10169	3.5302	0.041993
	Error	86421	30	2881		

Table A19. Summary of univariate tests of significance for glutathione (GSH) of *Halimeda macroloba*, *Halimeda opuntia*, and *Padina boryana* in responses to temperature and light treatments. Significant values ($p < 0.05$) are shown in bold

D. Glutathione (GSH)						
	Effect	SS	df	MS	F	p
<i>Halimeda macroloba</i>	Intercept	621980.4	1	621980.4	426.4743	0.000000
	Temperature	13229.0	2	6614.5	4.5354	0.021341
	Light	994.4	1	994.4	0.6818	0.417090
	Temperature*Light	573.2	2	286.6	0.1965	0.822911
	Error	35002.2	24	1458.4		
<i>Halimeda opuntia</i>	Intercept	534848.7	1	534848.7	614.7751	0.000000
	Temperature	2605.9	2	1302.9	1.4977	0.243823
	Light	465.3	1	465.3	0.5348	0.471667
	Temperature*Light	80.5	2	40.3	0.0463	0.954869
	Error	20879.8	24	870.0		
<i>Padina boryana</i>	Intercept	9964445	1	9964445	747.3292	0.000000
	Temperature	3643	2	1821	0.1366	0.872852
	Light	85106	1	85106	6.3829	0.017033
	Temperature*Light	2713	2	1357	0.1017	0.903566
	Error	400002	30	13333		